EXPERIMENTAL STUDIES ON TIG WELDING OF ADVANCED MATERIAL UNDER VARIOUS PARAMETERS

A Thesis Submitted
in Partial Fulfilment of the Requirements
for the Degree of

MASTER OF TECHNOLOGY

in

DESIGN ENGINEERING

by

Safraj Ansari
(Enrollment No. 1200456004)

Under the Supervision of

Dr. Amrit Anand Dosar

Asst. Professor

Department of Mechanical Engineering

Babu Banarsi Das University, Lucknow

BBD UNIVERSITY

to the

School of Engineering

BABU BANARASI DAS UNIVERSITY LUCKNOW

June, 2022

CERTIFICATE

It is certified that the work contained in this thesis entitled "**EXPERIMENTAL STUDIES ON TIG WELDING OF ADVANCED MATERIAL UNDER VARIOUS PARAMETERS**", by Safraj Ansari (Roll No. 1200456004), for the award of Master of Technology from Babu Banarasi Das University has been carried out under my/our supervision and that this work has not been submitted elsewhere for a degree.

Signature

Dr. Amrit Anand Dosar

(Assistant Professor)

Mechanical Engineering, BBD

University, Lucknow, U.P., India

Date:

EXPERIMENTAL STUDIES ON TIG WELDING OF ADVANCED MATERIAL UNDER VARIOUS PARAMETERS

Safraj Ansari

ABSTRACT

The material Stainless Steel (AISI 309) is extensively used in almost all types of the thermal power plant, petroleum industries, waste treatment industries etc. The material AISI 309 stainless steel is used as a specimen which is prepared by wire cut EDM process. The specimen dimension is tested as per the ASTM standard. Tungsten inert gas (TIG) welding is used to improve mechanical properties and to reduce the manufacturing costs, by the Taguchi`s experimental design method which is used for optimization. Three different welding process parameters such as welding current, welding speed and gas flow rate have selected to perform the experiments using L9 orthogonal array. The tensile strength, bending strength and Impact strength tests is conducted to check the final weld quality and welding current, welding speed and gas flow rate were accomplished at optimum welding current of 170 A, welding speed of 2 mm/min and gas flow rate of 15 L/min using Taguchi Method.

ACKNOWLEDGEMENTS

Achievement of one's goal is not a single person's effort but it is the advice, help, suggestions and blessings of many people. So, it gives me immense pleasure to express my gratitude, regards and acknowledgement to them. I express my deep sense of gratitude to Dr. Amrit Anand, (Assistant Professor) Mechanical Engineering, BBD University, Lucknow, U.P., India for their valuable guidance, keen interest and encouragement at various stages of the academic as well as training period. I am thankful Dr. Sunil Kumar for facilitating and taking the work under perusal during the entire session. It is a matter of great pleasure to express my wishes and genuine thanks to Er. Chandra Bhushan, Er. Ravi Vishwakarma, Er. Manoj Soni for their advice, support, help, and companionship throughout my project work. This project work is simply impossible without the support of my parents. I am indebted to my father and mother for their care and support. Last but not least, I am also grateful to all those who helped me knowingly or unknowingly in various ways in completion of my thesis work.

SAFRAJ ANSARI

TABLE OF CONTENTS

List of tables

List of figures

List of Symbols, abbreviations and Nomenclature

AISI: American Iron and Steel Institute.

ANOVA: Analysis of variance

ASTM: American Society for Testing and Materials

TIG: Tungsten inert gas

EDM: Electrical Discharge Machining

CNC: Computer Numerical Control

OA: Orthogonal Array

S/N: Signal-to-Noise ratios

UTM: Universal Testing Machine

WC: Welding Current

WS: Welding Speed

GFR: Gas flow Rate

C: Carbon

Si: Silica

Mn: Manganese

P: Phosphorus

S: Sulphur

N: Nitrogen

Cr: Chromium

Ni: Nickel

CHAPTER 1

1 INTRODUCTION

1.1. Material AISI 309 stainless steels:

Stainless steel (AISI 309) is extensively used in almost all types of thermal power plant, petroleum industries, waste treatment industries etc. This type of AISI 309 has high strength, weldability, toughness, ductility, excellent oxidization resistance and excellent formability. AISI 309 SS applications includes furnace parts, jet engine parts, heat exchangers, evaporators, chemical processing equipment, Automotive exhaust part, tanks, Fire box sheet and Other high temperature Containers. The chemical composition of AISI 309 is show in table 1. And material shown in fig. 1.1

Table 1 The chemical composition of AISI309

Grade	C%	Si%	Mn%	P%	S%	N%	Cr%	Ni%
309	0.067	0.26	1.73	0.036	0.003	-	22.15	12.19

Stainless Steel 309 is an austenitic stainless steel that's frequently utilised in high-temperature applications. Because of the high chromium and nickel content, it has comparable oxidation and corrosion resistance. 309 stainless steels can be machined in the same way that 304 stainless steels can. Grade 309 Stainless Steel can also be welded utilising the resistance and fusion method. Oxyacetylene welding is not advised for welding 347H stainless steel. The 309 stainless steel grade is heated to 1177°C, then reheated to 982°C before being quenched quickly. After-work annealing can be used to restore its corrosion resistance. If the work hardening rate of grade 309 stainless steel is high, it can be stamped, headed, upset, and drawn. After cold working, annealing is performed to minimise internal tension. After annealing at 1038-1121°C, 309 stainless steel is quenched in water. Cold working can improve the hardness and strength of 309 steel.

Fig. 1.1 Material (AISI 309 Stainless steel)

1.2. TIG Welding of AISI 309 stainless steel:

To improve the mechanical qualities of stainless steel, the tungsten inert gas (TIG) welding method is used. TIG welding produces a higher-quality, more accurate weld, a smaller heat affected zone, no slag, and fewer faults than other welding methods, hence it is extensively utilised. GTAW (Gas Tungsten Arc Welding) is an abbreviation for TIG welding, which uses a non-consumable tungsten electrode. The preparation of a high-quality weld is regarded as a difficult task. As a result, input parameters such as welding current, welding speed, gas flow rate, gas pressure, and so on can be used to manage welding quality. An electric arc is created between a tungsten electrode and the base metal in the TIG welding process. To protect the weldpool in the TIG welding process, an inert gas (argon-helium) shield is employed instead of a slag. TIG welding setup show in fig. 1.2.

The goal of this study is to conduct an experimental inquiry into optimizing TIG welding settings for AISI 309 plates. TIG welding is a conventional choice of welding process with a high level of joint quality. This type of AISI 309 has strong strength, excellent oxidation resistance, and outstanding formability. Further, The TIG welding procedure is optimized using optimization techniques. The weld joint's mechanical qualities were then tested. Based on the L9 Taguchi Orthogonal array design, 27 pairs of samples were welded using the TIG technique. This strategy improves design for superiority, performance, and cost in an efficient, modest, and deliberate manner.

Tungsten Inert Gas (TIG) welding fuses metal in the joint area and produces a molten weld pool by using the heat generated by an electric arc struck between a non-consumable tungsten electrode and the specimen. To safeguard the weld pool and non-consumable electrode, the arc area is encased in an inert or reducing gas shield. Filler can be introduced by introducing a consumable wire or rod into the established weld pool, or the process can be run autogenously (without filler). TIG welds a wide range of materials with thicknesses up to roughly 8 or 10mm and generates very high-quality welds. It works very well with sheet material.

The success of this welding process is dependent on a number of elements, including the shielding gas used, the welding wire used, the tungsten electrode used, and the welding technique used.

Fig. 1.2 Tig welding machine

1.2.1. Principle:

TIG welding works in the same way that arc welding does. TIG welding creates a high-intensity arc between the tungsten electrode and the work piece. The work piece is usually attached to the positive terminal, while the electrode is connected to the negative terminal. This arc generates heat energy, which is then used to fusion weld metal plates together. A shielding gas is also utilised to prevent oxidation of the weld surface.

It is a crucial aspect of TIG welding. The tungsten electrode, collets, and nozzle are the three primary components of this torch. Water or air cooling is available for this torch. The tungsten electrode is held in place by a collet in this torch. The diameter of these varies depending on the diameter of the tungsten electrode. The nozzle allows shielded gases and arc to pass into the welding zone. Because the nozzle cross section is small, the arc is very intense. At the nozzle, there are protected gas passages. Because of the existence of a powerful spark, the TIG nozzle must be replaced on a frequent basis.

As a shielding gas, argon or other inert gases are commonly utilised. The primary goal of shielding gas is to keep the weld from oxidising. The shielded gas prevents oxygen or other air from entering the welded zone. The choice of inert gas is determined by the metal to be welded. The flow of shielding gas into the welded zone is controlled by a mechanism.
Filler material is rarely needed when welding thin sheets. Filler material is used for thick welds. The filler material is in the form of rods that are manually fed into the weld zone.

1.2.2. Working:

First, the welding electrode or tungsten electrode receives a low voltage, high current feed from the power source. The electrode is usually connected to the negative terminal of the power source, while the work piece is attached to the positive terminal.
A spark between the tungsten electrode and the work piece provides the current. Tungsten is a non-consumable electrode that produces a powerful arc. The arc generated heat, which melted the base metals and formed the welding joint.
The welding torch is supplied with shielding gases such as argon and helium via a pressure valve and a regulating valve. These gases form a barrier that prevents oxygen and other reactive gases from entering the weld zone. These gases also produce plasma, which boosts the electric arc's heat capacity and consequently its welding capabilities.

Filler metal is not necessary for welding thin materials, but it is employed in the form of rods that are manually fed into the welding zone by the welder.

1.2.3. Different type of welding processes:

Based on the heat source used welding processes can be categorized as follows:

1.2.3.1. Arc Welding:

In the arc welding process, an electric power supply is used to create an arc between the electrode and the work-piece material, causing the work-piece metals to melt at the interface and allowing welding to take place. Arc welding can be done using either AC or DC electricity. Consumable and non-consumable arc welding electrodes are available. For non-consumable electrodes, an external filler material could be used.

1.2.3.2. Gas Welding:

In the gas welding process, a focused high-temperature flame produced by gas or gas mixture combustion is employed to melt the work components to be bonded. An external filler material is used to ensure effective welding. The most common type of gas welding is oxyacetylene gas welding, in which acetylene and oxygen react to produce heat.

1.2.3.3. Resistance Welding:

In resistance welding, heat is generated by the transfer of a considerable amount of current (1000–100,000 A) through the resistance created by the contact between two metal surfaces. The most common type of resistance welding is spot welding, which uses a pointed electrode. Continuous type spot resistance welding can be used for seam welding when a wheel-shaped electrode is used.

1.2.3.4. High Energy Beam Welding:

This type of welding uses a high-intensity concentrated energy source, such as a laser or an electron beam, to melt the work components and fuse them together. Precision welding, advanced material welding, and occasionally welding of different materials are all done with these sorts of welding, which are not achievable with ordinary welding procedures.

1.2.3.5. Solid-State Welding:

In solid-state welding processes, the materials to be joined are not melted. Other solid-state welding techniques include ultrasonic welding, explosion welding, electromagnetic pulse welding, friction welding, friction-stir welding, and others.

1.2.4. Arc Welding:

Arc welding is one of the most extensively utilised welding procedures for a variety of materials. The following are examples of arc welding processes:

1.2.4.1. Shielded Metal Arc Welding (SMAW) or Manual Metal Arc Welding:

This is the most common type of arc welding, in which a flux-coated consumable electrode is used. As the electrode melts, the flux disintegrates, releasing shielding gas to protect the weld region from ambient oxygen and other gases, as well as slag to cover the molten filler metal as it moves from the electrode to the weld pool. As the weld cures, the slag floats to the pool's surface, shielding the weld from the elements.

1.2.4.2. Gas Metal Arc Welding (GMAW) or Metal inert or active gas welding (MIG/MAG):

In this type of welding, a continuous and consumable wire electrode is used. A welding cannon delivers a shielding gas, usually argon or a mixture of argon and carbon dioxide, into the weld zone.

1.2.4.3. Gas Tungsten Arc Welding (GTAW) or Tungsten Inert Gas (TIG):

The GTAW or TIG welding process is an arc welding method that uses a non-replaceable tungsten electrode to make welds. The weld zone is shielded from the atmosphere by a shielding gas, commonly Argon or Helium, or a mixture of Argon and Helium. A filler metal can also be manually fed for appropriate welding. During WWII, the GTAW welding process, also known as TIG welding, was developed. The advent of the TIG welding technology has made it possible to weld difficult-to-weld materials like aluminium and magnesium. TIG welding power sources, like other welding systems, have progressed from simple transformers to highly digitally controlled power sources today.

1.2.5. Basic mechanism of TIG welding:

TIG welding is an arc welding technique that uses a non-consumable tungsten electrode to make welds. The weld region is shielded from the atmosphere by an inert shielding gas (argon or helium), and a filler metal is commonly used. Through a hand-piece or welding torch, electricity is delivered from the power source (rectifier) to a tungsten electrode put into the hand piece. A constant-current welding power supply creates an electric arc between the tungsten electrode and the work piece, which is then traversed by a column of highly ionised gas and metal vapours. The tungsten electrode and welding zone are shielded from the ambient air by inert gas. Temperatures of up to 20,000oC can be generated by an electric arc, which can be focussed to melt and merge two different materials. The weld pool can be used to connect the base metal with or without filler material. Fig. 1.3 shows a schematic diagram of TIG welding and the mechanism of TIG welding.

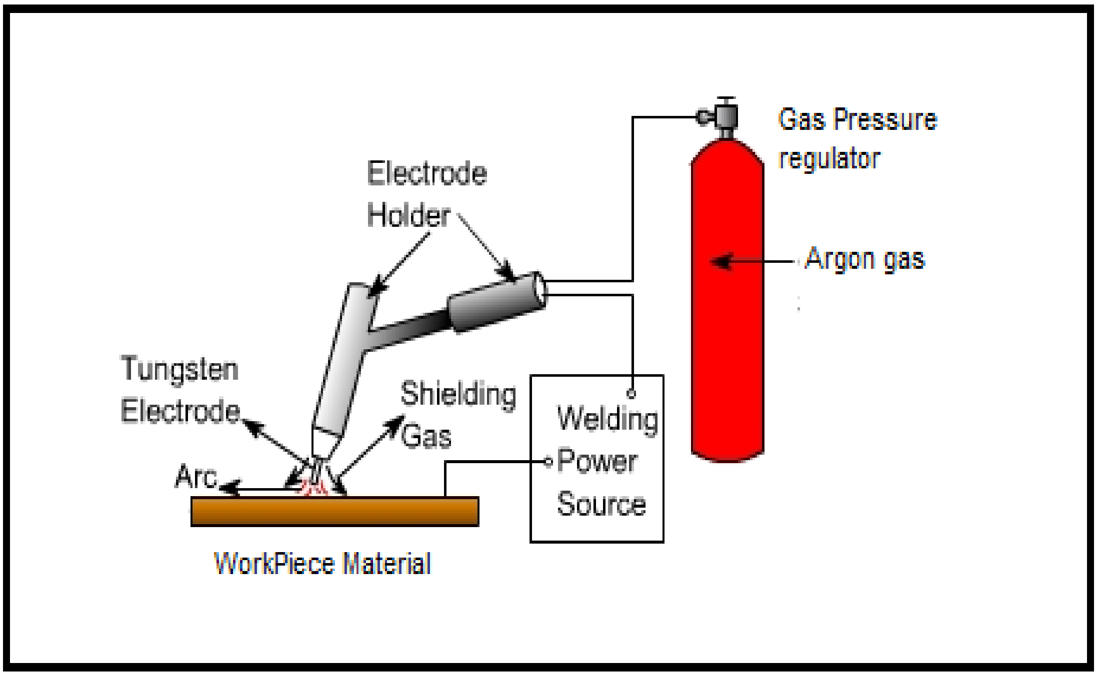

Fig. 1.3 mechanism of TIG welding

Tungsten electrodes are typically available in sizes ranging from 0.5 to 6.4 mm in diameter and 150 to 200 mm in length. The current carrying capability of an electrode is determined by whether it is attached to the negative or positive terminal of a DC power source. The power supply required to sustain the TIG arc has a drooping or constant current characteristic, which provides an effectively constant current output while the arc length is changed across many millimetres. As a result, natural variations in arc length have no effect on welding current in hand welding. When the electrode is short-circuited to the work piece, the ability to limit the current to the set value is also essential; otherwise, a very high current will flow, ruining the electrode. The power source's open circuit voltage is between 60 and 80 V.

1.2.6. Types of welding current used in TIG welding:

1.2.6.1. DCSP (Direct Current Straight Polarity):

In this technique of TIG welding, direct current is used. The tungsten electrode is attached to the power supply's negative end. This type of connection is the most common and commonly utilised DC welding process. If the tungsten is connected to the negative terminal, it will only get 30% of the welding energy (heat). The weld that results have a low profile and good penetration.

1.2.6.2. DCRP (Direct Current Reverse Polarity):

In this sort of TIG welding configuration, the tungsten electrode is connected to the positive terminal of the power source. Tungsten is quickly overheated and burned away since it absorbs the majority of the heat. DCRP has a shallow, wide profile and is often utilised at low amps on very light materials.

1.2.6.3. AC (Alternating Current):

This welding current is preferred by most white metals, such as aluminium and magnesium. The heat input to the tungsten is averaged out as the AC wave moves from one side to the other. Electrons migrate from the base material to the tungsten electrode when the tungsten electrode is positive on the half cycle. As a result, any oxide skin on the base material will lift. The waveform's cleaning half is referred to as such. As the wave progresses to the point where the tungsten electrode becomes negative, electrons will flow from the welding tungsten electrode to the base material. This section of the cycle is referred to as the penetration half of AC waveforms.

1.2.6.4. Alternating Current with Square Wave:

Thanks to modern energy advancements, AC welding machines may now be built using a wave form called as Square Wave. During the welding cycle, the square wave has better control, and each side of the wave can give greater cleaning and penetration.

1.2.7. Application:

TIG welding works best on metal plates that are 5 to 6 mm thick. TIG welding of thicker material plates can also be done in multiple passes, resulting in significant heat inputs and mechanical property deformation of the base metal. TIG welding gives you a lot of control over how much heat you put in and how much filler you put in, resulting in high-quality welds. Because TIG welding may be done in any position, it is suitable for tube and pipe junctions. TIG welding is a precise and clean process that requires little, if any, post-processing. This welding technology allows for both human and automated methods. In so-called high-tech industry applications like aerospace, TIG welding is commonly used.

1.2.8. Mostly used to weld aluminium and aluminium alloys:

- It is used to weld stainless steel, carbon base alloy, copper base alloy, nickel base alloy etc.
- It is used to welding dissimilar metals.
- It is mostly used in aerospace industries.
- Nuclear industry
- Food processing industry
- Maintenance and repair work
- Precision manufacturing industry
- Automobile industry

1.2.9. Advantage:

- TIG provides stronger joint compare to shield arc welding.
- The joint is more corrosion resistant and ductile.
- Wide verity of joint design can form.
- It doesn’t required flux.
- It can be easily automated.
- This welding is well suited for thin sheets.
- It provides good surface finish because negligible metal splatter or weld sparks that damage the surface.
- Flawless joint can be created due to non-consumable electrode.
- More control on welding parameter compare to other welding.
- Both AC and DC current can be used as power supply.
- Narrow concentrated arc

1.2.10. Disadvantage:

- Metal thickness to be weld is limited about 5 mm.
- It required high skill labour.
- Initial or setup cost is high compare to arc welding.
- It is a slow welding process.

1.2.11. Process parameters of TIG welding:

The following are the variables that influence the quality and outcome of the TIG welding process.

1.2.11.1. Welding Current:

Using a greater current for TIG welding could result in spatter and damage to the work piece. In TIG welding, lower current levels cause the filler wire to stick. Higher temperatures must be required for longer periods of time to deposit the same amount of filler materials, resulting in larger heat effected areas for lower welding current. The voltage is changed in fixed current mode to maintain the arc current constant.

1.2.11.2. Welding Voltage:

Welding The voltage may be fixed or adjustable, depending on the TIG welding equipment. A high starting voltage allows for faster arc initiation and a greater variety of operating tip distances. Too much voltage might result in a wide range in welding quality.

1.2.11.3. Inert Gases:

The shielding gas selection is influenced by the welding cost, weld temperature, arc stability, weld speed, splatter, electrode life, and other considerations. It also affects the penetration depth and surface profile of the final weld, as well as porosity, corrosion resistance, strength, hardness, and brittleness. Argon or Helium can both be used to properly TIG weld. To weld extremely thin materials, pure argon is employed. Argon arcs are usually smoother and quieter. When Argon is used instead of Helium, arc penetration is reduced. For these reasons, argon is preferred in most applications, with the exception of welding metals with high heat conductivity in larger thicknesses, which necessitates more heat and penetration. Helium can be used to weld relatively thick parts of metals with high heat conductivity, such as aluminium and copper. Pure argon can be used to weld structural steels, low alloyed steels, stainless steels, aluminium, copper, titanium, and magnesium.

An argon hydrogen mixture is used to weld some stainless steels and nickel alloys. Pure helium can be used to cure both aluminium and copper. Helium argon mixtures can improve low alloy steels, aluminium, and copper.

1.2.11.4. Welding speed:

TIG welding speed is an important factor to consider. When welding speed is increased, the amount of power or heat used per unit length of weld decreases, resulting in less weld reinforcement and penetration. Welding speed, sometimes called travel speed, is used to control the size and penetration of weld beads. It's entangled in the current. Fast welding speeds reduce wetting action and increase the chance of undercut, porosity, and irregular bead shapes, whereas slower welding speeds reduce porosity.

1.3. EDM Machine:

Electrical discharge machining is also known as spark machining or spark eroding. EDM is a machining technique in which an electrically charged single strand wire is continuously fed into a dielectric fluid (usually deionized water), and the resultant discharge is utilised to cut conductive material when the CNC is placed close to the grounded specimen. When the wire is pulled closer to the thing to be worked on, electric sparks cut (or rather, erode) through the metal. They are flushed and generally immersed in deionized water to remove impurities, cool the wire, and regulate the sparks. Fig. 1.4 shows this.

Fig. 1.4 EDM Machine

1.3.1. Type of EDM machine:

1. Wire Cutting Electrical Discharge Machining
2. Sinker Discharge Machining
3. Hole Drilling Electric Discharge Machining

1.3.2. Electrical Discharge Machining:

Discharge of Electric Machining is a process in which electrical energy is used to create a spark between the tool and the specimen, which allows material to be removed from the specimen's surface by local melting or vaporisation.

1.3.2.1. Working Principle of Electrical Discharge Machining Process:

The specimen is secured in the dielectric container using a fixture. The tool is fed by the Servo Feed Unit, which may move downward in a vertical direction. A positive connection attached to the specimen and a negative terminal connected to the tool power the electrical discharge machining process. Dielectric fluid is used to separate the tool and specimen, and the space between them is kept as narrow as feasible. Under normal circumstances, the dielectric fluid acts as an insulator, as previously stated. There is no electrical conductivity in this sense The dielectric fluid, on the other hand, ionises into Negative and Positive ions when enough pressure is applied. Heat is generated when positive ions attract negative ions and negative ions attract positive ions. A spark is formed between the tool and the specimen when positive and negative ions collide, allowing the material to be removed off the specimen's surface. The dielectric fluid reverts to an insulator when there is no spark in the container, and the technique for removing the material from the specimen's surface is repeated. This article provides a thorough explanation of the Electrical Discharge Machining process, including terms and how it works.

1.3.2.2. Parts of Electrical Discharge Machining:

The Electrical Discharge Machining (EDM) setup consists of

1. Pulse Generator (Power Supply)
2. Specimen
3. Fixture
4. Dielectric Fluid
5. Pump

6. Filter
7. Tool Holder
8. Spark generation
9. Tool

1. **Pulse Generator (Power Supply):** The EDM process is powered by a negative terminal connected to the tool and a positive terminal connected to the work piece.
2. **Work piece:** A fixture is used to secure the work piece in the dielectric container, and the positive terminal of the power supply is connected to it.
3. **Fixture:** The fixture is used to hold the work piece properly in a dielectric container.
4. **Dielectric Fluid:** The work piece and the tool are separated using dielectric fluid, and the gap between them is kept as small as possible. The dielectric fluid acts as an insulator under normal circumstances. In this sense, there is no electrical conductivity. However, when high pressure is applied, the dielectric fluid ionises into Negative and Positive Ions, allowing it to conduct.
5. **Pump:** A pump is used to send the dielectric fluid from the base of the container to the tool and work piece such that more MRR takes place.
6. **Filter:** A filter was situated just above the pump to remove any irregularities or dust particles present in the dielectric medium.
7. **Tool** Holder: It is used to hold the tool properly.
8. **Spark generation:** A spark is generated between the tool and work piece in the presence of dielectric medium and thereby material removal takes place from the surface of work piece.
9. **Tool:** The tool used in the Electric Discharge Machining process is either Copper or Tungsten or Copper-Tungsten Alloy.

1.3.3. Properties of the Dielectric Fluid/Medium:

- Low viscosity.
- Remain electrically non-conductive up to the desired voltage breakdown takes place.
- It can act as a good cooling medium.

- It can carry away all the metal particles produced during the spark erosion.

Electrolyte used: Kerosene acts as a Dielectric Fluid in Electrical Discharge Machining process.

Optimum Gap: The Optimum gap between the tool and the work piece is 0.03 mm.

And using Voltage - 70V.

1.3.4. Applications of Electro Discharge Machining:

- Drilling for micro holes in the nozzle.
- This is used in thread cutting.
- Used in wire cutting.
- Rotary form cutting.
- Helical profile milling.
- Curved hole drilling.
- Engraving operation on harder materials.
- Cutting off operation.
- The shaping of alloy steel and tungsten carbide dies.

1.3.5. Advantages of Electrical Discharge Machining:

- It can be used for any hard material and even in the heat-treated condition.
- Any complicated shapes made on the tool can be reproduced.
- High accuracy of about 0.005 mm can be achieved.
- Good surface finish can be achieved economically up to 0.2 microns.
- Machining time is less than the conventional machining process.
- No mechanical stresses are developed in this process (There is no contact between tool and work)
- Higher tool life due to proper lubrication and cooling.
- Hard and erosion resistant surface on the dies can be developed easily.
- It can be applied to any electrically conductive materials.

1.3.6. Disadvantages of Electrical Discharge Machining:

- High power consumption.
- The sharp corner cannot be reproduced.
- High heat developing causing the change in metallurgical properties of materials.
- The workpiece must be an electrical conductor.
- Surface cracking may take place in some materials.
- Redressing of a tool is required for deep holes.
- Over-cut is formed.
- Difficult finding expert machinists.
- Workpiece material must be electrically conductive.
- Perfect square corner holes are not possible to produce.
- Hardening of the workpiece is taking place near to the hole.

1.4. Tensile Test:

Tensile tests are performed to see how materials react when they are pulled taut. To evaluate the UTS of a material, a sample is generally yanked to its breaking point in a basic tensile test. Tensile tests are performed to see how materials react when they are pulled taut. To evaluate the ultimate tensile strength of a material, a sample is generally yanked to its breaking point in a basic tensile test. The amount of force (F) and elongation (L) applied to the sample are measured during the test. Material properties are described using two concepts: stress (force per unit area) and strain (percent change in length). Stress (= F/A) is calculated by dividing the force values by the cross-sectional area of the sample. Strain is computed by dividing the change in length by the initial length of the sample (= L/L). These figures are then plotted on an XY plot of a stress-strain curve. Several testing and measurement procedures are utilised depending on the chemical being assessed and its intended application.

Tensile strength is the amount of strain or stress that a material can endure before stretching and breaking. Tensile strength, as the name indicates, is a material's resistance to tension caused by mechanical stresses. The ability of materials used for structural purposes to resist breaking under tensile stress is one of the most essential and widely assessed properties. UTM Machine for Tensile Test shown in fig. 1.5.

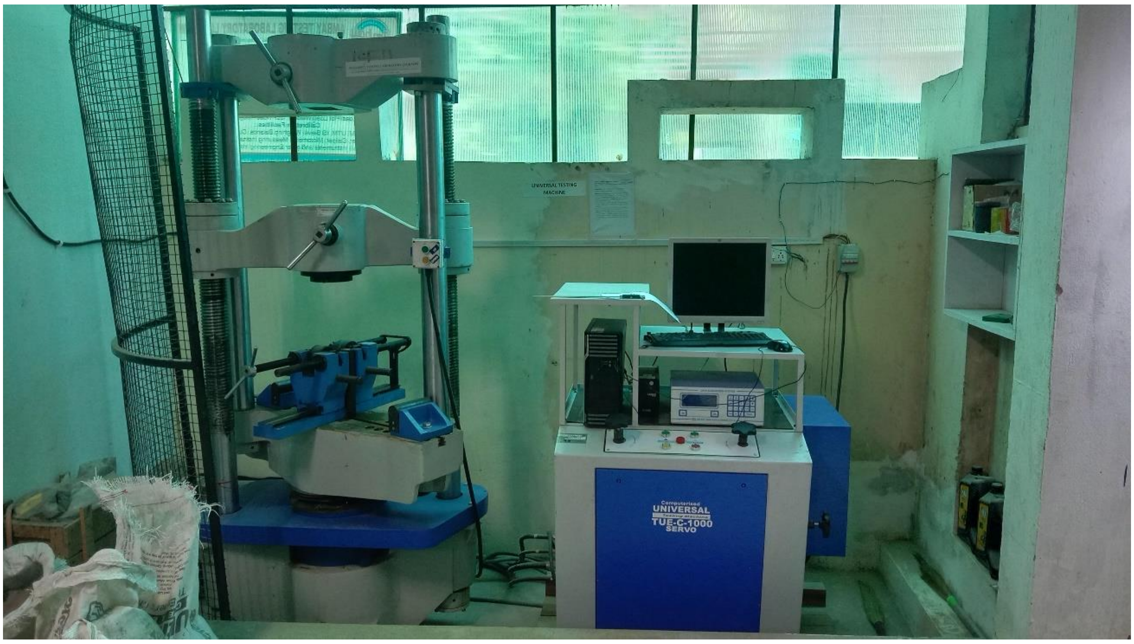

Fig. 1.5 UTM Machine for Tensile Test

There are three types of tensile strength:

Yield strength – The stress a material can withstand without permanent deformation

Ultimate strength – The maximum stress a material can withstand

Breaking strength – The stress coordinate on the stress-strain curve at the point of rupture

1.5. Bending Test:

Bending strength is described as a material's ability to withstand deformation under load, and it indicates the material's greatest stress at the time of rupture. Bending tests are divided into two categories. There are two types of bending tests: three-point bending and four-point bending. In a three-point bending test, the uniform stress region is relatively small and concentrated under the centre loading point. The area of uniform stress lies between the inner span loading points in a four-point bending test (typically half the outer span length). UTM Machine for Bending Test shown in fig. 1.6.

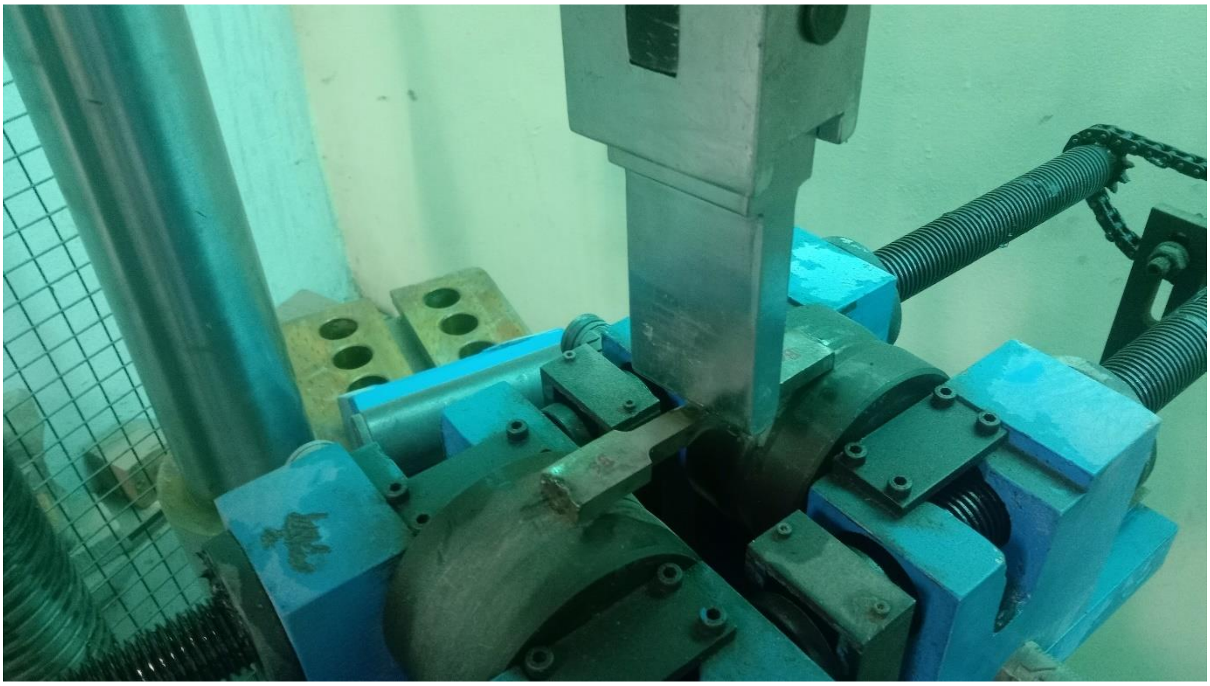

Fig. 1.6 UTM Machine for Bending Test

When a specimen is bent, it is subjected to a variety of stresses across its length. The stress will be at its highest compressive value near the concave face's edge. The specimen's stress will be at its highest tensile value at the convex face. Because most materials fail under tensile stress before compressive stress, the specimen's flexural strength is the greatest tensile stress that can be endured before it fails. If the material were homogeneous, the flexural strength would be the same as the tensile strength. As a result, a specimen's flexural properties are determined by the combined influence of all three stresses, as well as (to a lesser extent) the specimen's geometry and the rate at which the load is applied. Bend testing gives information about a material's modulus of elasticity and bending strength.

1.6. Impact test:

As indicated in Fig. 1, the specimen is placed across the lowest point in the path of a striker installed at the end of a pendulum. After being elevated to a predetermined height h1 and then released, the striker swings against the specimen and smashes it. The striker swings to the other side of the specimen, reaching a height of h2. The amount of energy absorbed in fracture is clearly equal to the difference between the two heights multiplied by the striker's weight. Impact testing Machine for Impact test shown in fig. 1.7 and Specimen clamped for Impact Test shown in fig. 1.8.

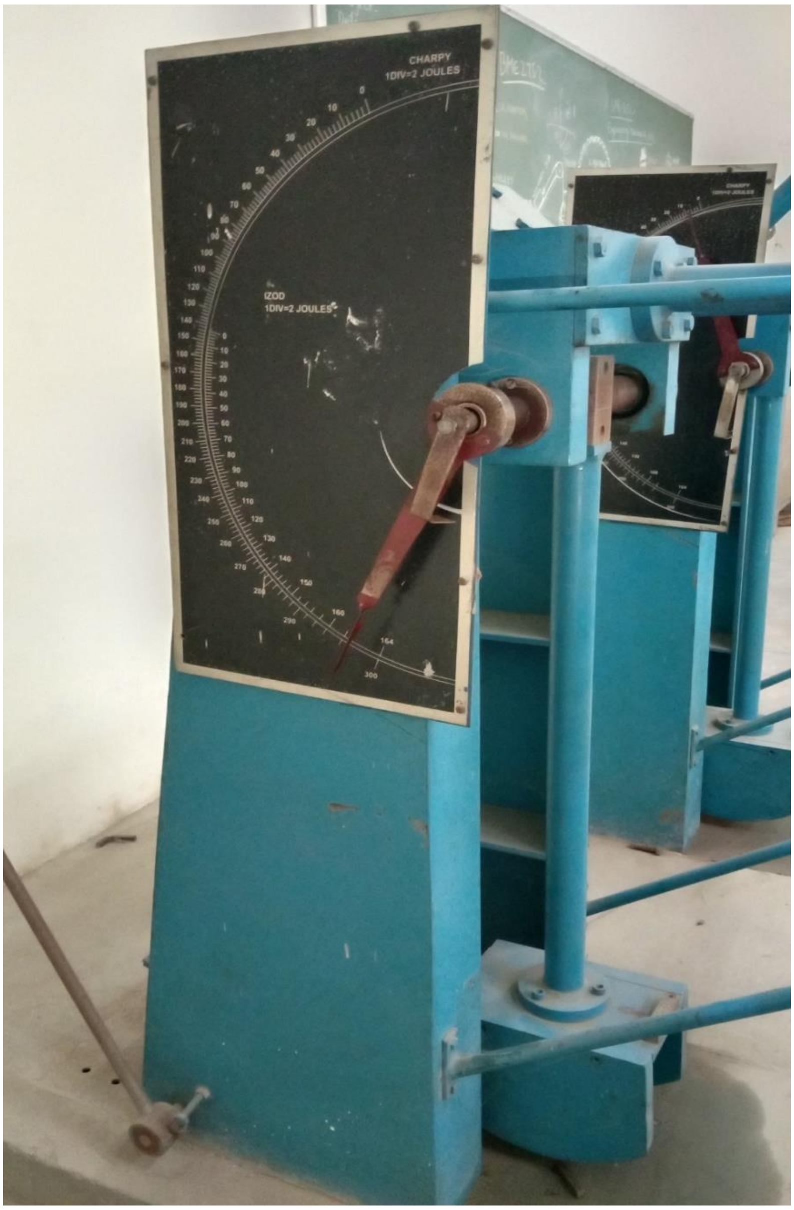

Fig. 1.7 Izod testing Machine for Impact test

Fig. 1.8 Specimen clamped for Impact Test

The test piece in the Izod impact test is a cantilever that is clamped vertically in an anvil and has a V notch at the top of the clamp. The test item is struck by a striker suspended on a pendulum that is free to fall from a fixed height, producing a 120 ft lb energy blow. After breaking the test piece, a slave friction pointer attached on the dial records the height to which the pendulum rises, from which the absorbed energy quantity is calculated.

1.7. Introduction to taguchi method:

1.7.1. Design of experiments:

A well-planned series of experiments in which all important variables are varied throughout a predefined range is a considerably better technique to obtain systematic data. Mathematically, such a large number of experiments should produce the desired results. Typically, the number of tests and resources (materials and time) required are excessive. The researcher will typically do a subset of the whole set of experiments to save time and money. It's doesn't, however, lend itself to a simple understanding of the science behind the event. The influence of various factors on observed data are not clearly evident since the analysis is complicated (though it may be straightforward for a mathematician or statistician). The approach does not always provide the optimum parameter choices, particularly when considerable optimization is necessary. A good illustration of the drawbacks of design of experiments is the planning of a world cup event, such as football. While all matches are well-organized in terms of the various teams and locations on various days, the planning is careless with the match's outcome (win or lose)!!!! Obviously, such a method is unsuited for doing scientific research (save for coordinating multiple institutions, committees, people, and equipment, materials etc.).

1.7.2. Taguchi Method:

Dr. Taguchi of the Nippon Telephone and Telegraph Company in Japan has devised a method based on "ORTHOGONAL ARRAY" tests that results in considerably lower "variance" for the experiment when the control parameters are "optimised." The Taguchi Method thus combines Design of Experiments with optimization of control parameters to produce the best results. The Signal-to-Noise ratios (S/N) developed by Dr. Taguchi, which are log functions of desired output, serve as objective functions for optimization, data analysis, and prediction of optimal outcomes. A P-Diagram, as illustrated below, is the easiest way to explain this ("P" stands for Process or Product). Although noise is present in the process, it should have no impact on the outcome! The major goal of the Taguchi experiments is to reduce output variances even when noise is present in the process. The procedure is then described as ROBUST. Shown in fig. 1.9.

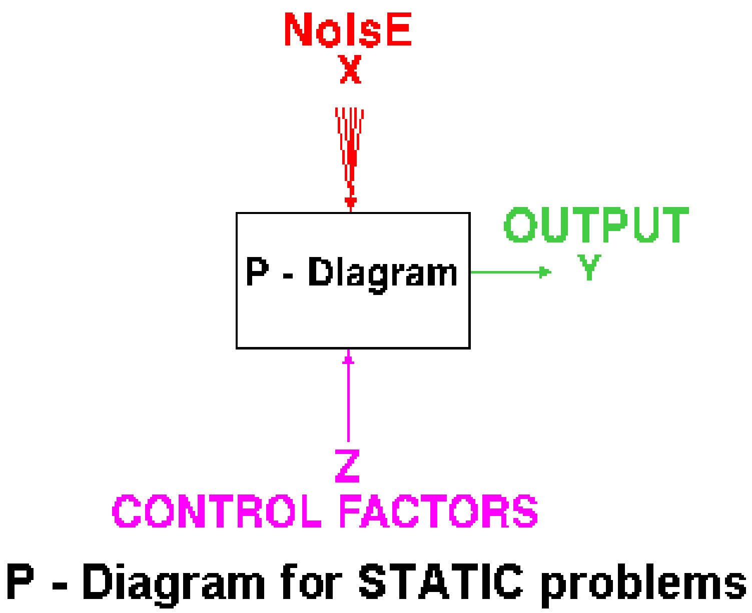

Fig. 1.9 Signal-to-Noise ratios

1.7.2.1. There are 3 Signal-to-Noise ratios of common interest for optimization: -

1. **SMALLER-THE-BETTER:**

n = -10 Log10 [mean of sum of squares of measured data]

This is the standard S/N ratio for all unwanted qualities, such as "defects," for which zero is the ideal value. Furthermore, The discrepancy between measured data and ideal value is anticipated to be as minimal as feasible when an ideal value is finite and its maximum or minimum value is established (for example, maximum purity is %, maximum Tc is 92K, and the minimum time to create a cable is 1 sec). The general form of the S/N ratio is then,

n = -10 Log10 [mean of sum of squares of {measured - ideal}]

2. **LARGER-THE-BETTER:**

n = -10 Log10 [mean of sum squares of reciprocal of measured data]

By taking the reciprocals of measured data and then the S/N ratio as in the smaller-the-better instance, this case has been changed to SMALLER-THE-BETTER.

3. **NOMINAL-THE-BEST:**

This case arises when a specified value is MOST desired, meaning that neither a smaller nor a larger value is desirable.

Examples are;

(i) Most parts in mechanical fittings have dimensions which are nominal-the-best type.

(ii) Ratios of chemicals or mixtures are nominally the best type.

e.g. Aqua regia 1:3 of HNO3: HCL
Ratio of Sulphur, KNO3 and Carbon in gun powder

(iii) Thickness should be uniform in deposition /growth /plating /etching.

1.8. ANOVA:

Analysis of variance (abbreviated as ANOVA) is a very helpful tool in economics, biology, education, psychology, sociology, and business/industry research, as well as in a variety of other areas. When there are several sample cases, this strategy is employed. As previously stated, the z-test or the t-test can be used to determine the significance of a difference between the means of two samples, but the problem occurs when we want to look at the significance of a difference between more than two sample means at the same time. The ANOVA technique allows us to execute this simultaneous test and is thus regarded as a valuable analytical tool in the hands of a researcher. This technique can be used to determine whether the samples were taken from populations with the same mean. The ANOVA technique is useful in instances where we need to compare more than two populations, such as comparing agricultural production from multiple varieties of seeds, gasoline mileage from four autos, smoking behaviours of five groups of university students, and so on. In such cases, it is often not desirable to analyse all conceivable combinations of two populations at the same time, as this would necessitate a large number of tests before we could make a judgement. This would take a lot of time and money, and even then, some relationships might get undiscovered (particularly the interaction effects). As a result, the ANOVA technique is frequently used to study variations among the means of all populations at the same time.

1.9. Minitab:

Minitab is a statistics tool created by some researchers to assist six sigma experts in analysing and interpreting data to aid in the business process. The data input has been simplified to make it easier to use for statistical analysis and to manipulate the dataset. If trends, patterns, or charts are provided, they are evaluated and interpreted in order to reach a final decision. The responses are offered, and they are amplified with the products or services provided to assist in the business. The Minitab tool makes problem-solving simple and quick.

Fig. 1.10 Minitab 19

CHAPTER 2

2 LITERATURE REVIEW

Shanmugasundar et al., (2019) reviewed that TIG welding processes improve the quality of a welded material of austenitic stainless steel (AISI 304l). Tungsten inert gas (TIG) has been used in this welding process and optimized the outcome on the basis of welding current, gas flow rate and nozzle to work piece distance.

Natrayan et al., (2020) denoted that utilised the taguchi method to optimize the quality of wielded joint with the help of control parameters like welding current, weld speed, filler diameter for tensile strength. The tests were performed by using l9orthogonal array. A regression model was established a link between welding input parameters and penetration for tungsten inert gas. This research concludes that the exceptional process parameters for tensile strength at level 1 (a1), weld speed at level 3 (b3), filler diameter at level 3 (c3) and the outcomes were determined by ANOVA which shows that wielding speed is the major factor to improve the tensile strength.

Vinoth et al., (2021) focused on the optimization of the input parameters like welding speed, current, and gas flow rate and used TIG welding technique on 316 stainless steels through taguchi's method. The response parameters are tensile strength, impact strength and corrosion rate. The values of input parameters were optimized and evaluated to get desired mechanical properties which was welding speed of 190 mm/min, welding current of 150 amp and gas flow rate of 15 ltr/min using taguchi based grey relational analysis method.

Kumar et al., (2019) described the mechanical properties of the weld structure and the welding parameters of TIG welding process needs to be optimized to reduce the manufacturing costs. The present investigation points the optimization of the procedure parameters of TIG joining procedure. AISI 304 materials selected as a base metal. The dimension of sample is 200 mm × 50 mm × 3 mm. The sample was welded by the TIG welding method. The selection of input parameters was based on their significant effect of the weld sample mechanical properties. The selected input parameters are voltage, current, gas flow and root gap. 27 tests were carried out, which was designed by taguchi's L27 orthogonal array by using 4 factors and 3 levels using minitab-17software. By conducting the tensile strength test checks the final weld quality.

Avinash et al., (2019) worked on pcgta welding process for joining of two dissimilar plates, on steel grade 304 and monel 400, by employing ernicrmo-3 as filler. For designing and analysing experimental outcomes for improving the welding quality characteristics, taguchi method was used. For designing of process parameters an l-9 orthogonal array is used for optimizing the mechanical properties and heat affected region of base metals. Analysis of variance (ANOVA) has also been used for compiling and describing the outcomes in mathematical terms.

Ahmad et al., (2019) focused on process parameters optimization of tungsten inert gas (TIG). Taguchi method is very effective and efficient to solve the process parameters optimization problem to the find optimum processing parameters, but it is found that the traditional taguchi method is not sufficient to solve the problem with multi response problem to get optimum outcomes and to face the global challenges of the producers as it is impractical to obtain more than one exceptional processing parameters through taguchi. In order to survive in the global market it is necessary to used advanced and modified optimization techniques.

Jayashree et al., (2019) worked on 6061al alloy which is so strong and hence used in aggressive conditions like aerospace applications. In order to prevent from various defects like porosity, hot cracking and stress corrosion cracking during welding of aluminium alloy have to be optimized. Tungsten inert gas (TIG) welding of 6061al alloy has been done which is based on taguchi's design of tests by l9 orthogonal array.

Mishra et al., (2019) used two different sheet of metal of different grades of stainless steel 310 and 304 of 3 mm thickness and TIG welded with single and double 'v' butt joint. Two gas tungsten arc weld joint was produced by opting the current as 110 amp and voltage 19 v. Two shielded metal arc weld joints were produced when the current was kept as 80 amp and voltage 19 v. The welded samples were evaluated by dye penetrant inspection to identify the weld defects. From the inspection of weld samples, it was found defect free from cracks, porosity, lack of penetration and etc. The welded samples were tested for tensile and found as maximum 594 mpa in the case double 'v' shielded metal arc welded joint and 556 mpa in the case of double ‘v’ butt joint by the gas tungsten arc welding process. The research work will be helpful to choose effective welding technique of different alloys of stainless-steel grades 310 and 304 of 3 mm thickness with single or double ‘v’ edges for the practical use.

Ramana et al., (2019) focussed on high frequency technology i.e., robot tungsten inert gas welding of work pieces. The process parameters capture important role in successful welding of dissimilar materials. The response surface methodology has been used by changing weld control parameters for optimization. For each weld, the impact strength was measured. To maximize the impact strength of weld joints, the control parameters are to be optimized. This study revealed that current of 180-amp, 0.08 mm/min travelling speed and 0.82 mm/min wire feed rate are found to be optimum parameters to maximize the impact strength.

Chandrasekaran et al., (2017) investigated the weld strength of inconel 825 using gas tungsten arc welding (gtaw) process. The material which has high strength and corrosion resistant was always been a challenge for the researcher scholars. A box-behnken design of 27 experimental runs was performed. Further full quadratic models were prepared to study different welding responses. The predictive performance of the model shows an average percentage error as 6.72% for uts, 2.79% for ys and 17.75% for % e. Welding current (i) was found to be the most significant process parameters followed by welding speed (v) for each response. After optimization, the process parameters using desirability graphical analysis with maximum desirability value of 0.7089 was achieved.

Modenesi et al., (2000) gas tungsten arc welding is fundamental in those applications where it is important to control the weld bead shape and the metallurgical characteristics. ATIG welding uses a thin layer of an active ux that outcomes in a great increase in weld penetration. This effect is connected to the capture of electrons in the outer parts of the arc by elements of high electronegativity, which will constrict the arc. The changes in weld geometry were compared to variations in the electrical signals from the arc and the arc shape. The effect of the ¯ux on the weld microstructure was also studied. The outcomes indicate that even the very simple ¯ux that was used can greatly increase the penetration of the weld bead.

Manurunget al., (2012), reviewed an alternate method to optimize process parameters of resistant spot welding (RSW) towards weld zone development. The optimization method was attempted to consider the multiple quality characteristics i.e. namely heat affected zone (HAZ) and weld nugget by using multi-objective Taguchi method. The test was conducted on plate thickness of 1.5 mm for different weld current, hold time and weld time. The optimum value was analysed by means of MTM, which involved the calculation of total normalized quality loss and multi signal to noise ratio. A significant level of the welding parameters was further achieved by using the analysis of variance (ANOVA). Further, the first order model for prediction of the weld zone development was derived by using response surface methodology (RSM). Based on the experimental test, the proposed method can be effectively applied to estimate the size of weld zone.

Krishnan et al., (2014) done experiment to analyse the microstructure and oxidation resistance at different regions in the mild steel weld by TIG welding. Due to the complicated heat cycle and quick solidification, a dramatic change in the microstructure was noticed throughout the welding process. The mild steel weld's mechanical characteristics and oxidation resistance are also affected by this microstructure change. On 12 mm thick mild steel, autogenous TIG welding was done with 200 A current, 19 V voltage, and a welding speed of 100 mm/min. At the weld metal and heat affected zone, the grain size was finer.

Raj and Varghese et al., (2014) predict the distortion developed during TIG welding of low carbon steel. They constructed three-dimensional finite element models for longitudinal, angular, and transverse distortion in their research. Welding distortion caused by non-uniform heating and cooling. Welding current 150 A, electrode gap 3 mm, gas flow rate 25 l/min, electrode diameter 0.8 mm, and Argon as shielding gas were used to verify the model. In comparison to the other two directions, the highest deformation occurs on the surface opposing the weld and along the X direction of the weld.

Abhulimen and Achebo et al., (2014) performed experiments to identify the economical welding parameters using Response surface methodology (RSM) during TIG welding of mild steel pipe. Gas flow rate was 25 to 30 l/min, welding current was 130 to 180 A, arc voltage was 10.5 to 13.5 volt, and argon was used as a shielding gas. The highest tensile and yield strength of mild steel were attained utilising TIG welding, with results of 542 MPa and 547 MPa, respectively.

Mishra et al., (2014) have done comparison of mechanical properties between TIG and MIG welded dissimilar joints. Dissimilar material joints made of mild steel and stainless steel are quite frequent in structural applications. These dissimilar couplings offer an excellent balance of mechanical qualities, such as corrosion resistance and tensile strength, at a cheaper cost. MIG welding settings included welding currents of 80-400 A and voltages of 26-56 volts. TIG welding was done using a current of 50-76 amps and a voltage of 10-14 volts. Because there is less porosity in TIG welded dissimilar joints, they have a higher tensile strength. For TIG and MIG welding, both dissimilar joints offer the best ductility and yield strength.

Fujii et al., (2008) developed an advanced activated TIG welding method for deep penetration of weld joint. Surface tension gradient induces Maragoni convection on the molten pool. A little quantity of oxidising gas was utilised to regulate Maragoni convection. Welding current was 160 A, welding speed was 0.75 mm/s, electrode gap was 1mm, and Ar-O2 shielding gas was used. Maragoni convection shifts from interior to outward, and the weld form becomes wider and shallower.

Kuo et al., (2011) investigate effect of oxide fluxes during TIG welding of 6 mm thick dissimilar joint between mild steel and stainless steel. Powdered Cao, Fe2O3, Cr2O3, and SiO2 fluxes were utilised. To make paint, these granules were combined with acetone. A tiny coating of flux was sprinkled over the surface of the to-be-welded junction before welding. TIG welding was done at a speed of 150 mm/min, with a welding current of 200 A and a gas flow of 12 l/min. The results show that residual slag generated on the surface of TIG welds made using oxide flux. The use of SiO2 flux powder in TIG welding can improve joint penetration and weld to depth ratio.

Vikesh et al., (2013) studied the effect of activated flux on TIG welding process. They concentrated on the impact of TIG welding penetration in mild steel. In comparison to other arc welding processes, it has a shallow penetration depth. To avoid this, an activating flux powder is needed. When applying the activating TIG welding method on mild steel, Taguchi optimization is performed to optimise welding process parameters. Experiments show that increasing the weld current enhances the depth of penetration at the weld zone. The travel speed is inversely proportional to the depth of penetration.

Pal and Kumar et al., (2014) studied the effect of activated TIG welding on wear properties and dilution percentage in medium carbon steel welds of 12 mm thick plate. Powdered

TiO_2 and Cr_2O_3 fluxes were utilised. Flux powder was mixed evenly with acetone and rubbed onto the surface of the to-be-welded junction. With continuous welding speed, DC current and straight polarity were employed. With a welding current of 180A, a single pass TIG welding was done. In comparison to Cr_2O_3 flux coated weld, the TiO_2 flux coated weld enhanced the dilution on the base metal.

Nayee et al., (2014) studied the effect of oxide-based fluxes on metallurgical and mechanical properties of weld joint. With activating flux, tungsten inert gas welding is utilised to form welds between 6mm thick mild steel and stainless-steel plate. Powders of ZnO, TiO_2, and MnO_2 were employed in this study. Welding was done at a speed of 55 mm/min with a welding current of 200 A, an arc voltage of 12.5 V, and a welding current of 200 A. When compared to traditional TIG welding, TiO_2 and ZnO fluxes have the highest width to depth ratio. TiO_2 has the least angular deformation of the three fluxes.

Ruckert et al., (2014) show that during TIG welding process application of activated fluxes improve weld penetration and process competitiveness. They summarise the research on TIG welding with activating flux of stainless steel, plain carbon steel, aluminium, and titanium. The welding procedure was carried out using a current of 150 A and 175 A and a welding speed of 15 cm/min. Fluoride-based fluxes were shown to contribute to increased titanium and SiO_2 flux weld penetrations in stainless steel, plain carbon steel, and aluminium. The relevance of flux uniformity, flux composition, and profile in affecting the width to depth ratio of a weld is demonstrated.

Dhanda et al., (2014) done experiment to show the effect of activated fluxes on mild steel welds. TIG welding in autogenous mode can weld stainless steel and carbon steel plates up to 2 to 3 mm thick. The activating flux welding technique is seen to be a viable option for improving process productivity. The workpiece is made of Grade 91 steel. To generate a bead on plate weld, TIG welding was utilised on P91 steel using oxide powders CaO, ZnO, Fe_2O_3, TiO_2, MnO_2, and CrO_3 as flux material. This approach results in a greater depth of penetration as well as a smaller weld width. The use of activated fluxes enhanced the heat intake.

Fujii et al., (2006) done comparative study of strength characteristics of mild steel and cast iron weld using various welding process. The capacity of attaching cast iron to mild steel via the welding technique would be a significant contribution to the fabrication sector. Welding experts and trained welding operators in industrial welding helped choose welding procedures and consumables. For the manufacture of specimens, four frequently used welding procedures (Gas welding, metal arc welding with a covered electrode, Metal Active Gas welding, and TIG welding) were eventually chosen. Metal active gas welding produces test specimens with excellent elongation and tensile strength.

Mahajan et al., (2012) studied the effect of mechanical arc oscillation on the weld metal grain structure in mild steel using TIG welding. Columnar grain was detected in the weld without arc oscillation and smaller sized grain was observed in the weld with arc oscillation for the same welding settings. Various welding factors, such as arc voltage, welding current, welding speed, and welding process types, have an impact on the grain structure of mild steel welds. When comparing the strength of a weld with and without arc oscillation, it was discovered that the weld with oscillation had a greater strength. The hardness of the weld specimen with arc oscillation was lower than the hardness of the weld specimen without arc oscillation.

Pasupathy and Ravisankar et al., (2013) have done optimization of tungsten inert gas welding parameters using Taguchi technique for dissimilar joint of low carbon steel and aluminium. In order to optimise the process, welding current, welding speed, and the distance between the work material and the electrode were employed as input parameters in three levels.

Dye et al., (2014) observe quasi steady state phase evolution and transient stresses produced around the TIG welding torch in plain carbon steel during TIG welding process. Tubes with a diameter of 203 mm and a thickness of 3.2 mm were used. TIG welding was carried out in autogenous mode and under DCEN conditions. 35 A current, 14 V voltage, and 0.5 mm/s welding speed were the input welding parameters. This approach is also used to identify materials where the stress state has to be changed to prevent cracking. Experiment indicates that there is compression in the HAZ right behind the TIG welding flame.

Nasiri et al., (2014) done experiment to determine arc efficiency of TIG welding by calorimetric method. The arc efficiency was measured using a water-cooled calorimeter. On mild steel, TIG welding was done with two polarities (DCEN and DCEP) with a 5 mm arc length. The heat transfer from the workpiece to the water is the basis of the water-cooled technique. TIG welding was performed with a current DC power supply of 250 A. The effectiveness of the arc reduces as the arc length increases, according to the findings of the experiments. Gas flow rate has little effect on arc efficiency. It's also unaffected by welding current.

Meng et al., (2014) performed experiment to obtain high welding speed by using TIG and metal active gas (MAG) hybrid arc welding of mid steel. An orthogonal experiment was used to investigate the influence of welding settings on weld appearance and speed. The welded specimen's mechanical characteristics and microstructure were examined. These specimens were compared to MAG welds that are commonly used. On a 2.5 mm thick mild steel plate, a hybrid arc welding procedure was carried out with a welding current of 350 A and a gas flow rate of 9.5 l/min. In the case of a high-quality weld, hybrid arc welding may attain a welding speed of 3.5 m/min. The mechanical properties of a hybrid arc weld are superior to those of a traditional MAG weld.

Kuang et al., (2013) performed experiment to investigate the effect of oxide-based flux on 8 mm thick austenitic stainless-steel plate. They illustrate how welding distortion, hardness, ferrite number, and weld penetration depth are affected. SiO2 flux is blended with acetone and bead plate paint in powder form. This approach can enhance the depth of penetration at the weld zone, according to the testing results. Due to the high temperature of the junction, the hardness value of the weld rose. Welding distortion was greater in the autogenous mode, however angular distortion of the weld sample appears to be minimised with the use of flux.

CHAPTER 3

3 MATERIAL AND METHODOLOGY

3.1. Material:

AISI 309 SS has been used as a metal piece having the following dimensions, (length 120 mm, width 20 mm and thickness 10 mm) (120 X 20 X 10 mm), material sample shown in fig. 3.1. AISI 309 SS applications includes furnace parts, jet engine parts, heat exchangers, evaporators, chemical processing equipment, Automotive exhaust part, tanks, Fire box sheet and Other high temperature Containers. And experimental methodology Shown in fig. 3.2.

Fig. 3.1 Before EDM process Specimen

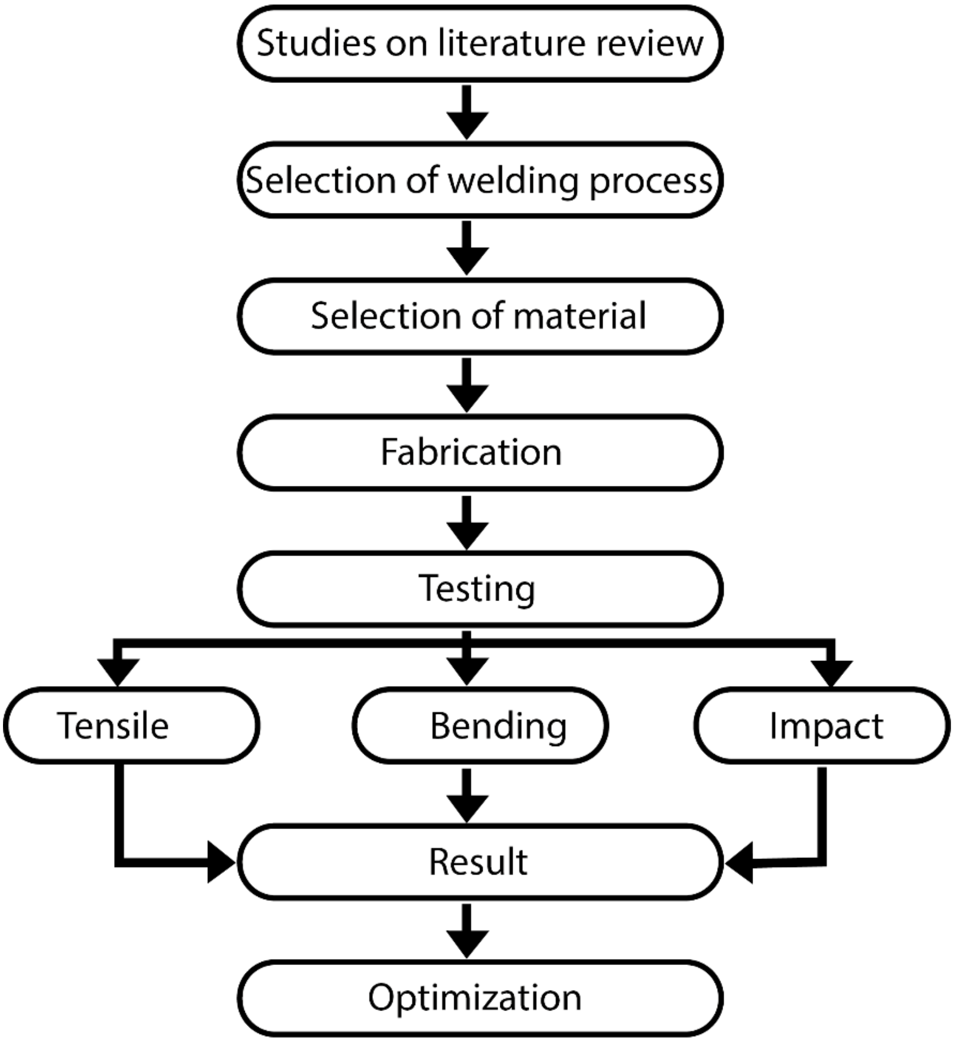

Fig. 3.2 Experimental Methodology

3.2. EDM Process:

Spark eroding or spark machining are terms used to describe electrical discharge machining. EDM is a machining technology that creates an electrically charged single strand wire that is continually supplied inside a dielectric fluid (typically deionized water), with the resultant discharge being utilised to cut conductive material when presented by the CNC near the grounded specimen. Electric sparks are created by moving the wire closer to the component being worked on, cutting or rather eroding the metal. To remove the particles, cool the wire to prevent breakage, and manage the sparks, they are flushed and generally bathed in deionized water. Test specimen diagram is shown in Fig. 3.3. and testing sample shown in fig. 3.4. and EDM wire cut shown in fig. 3.5.

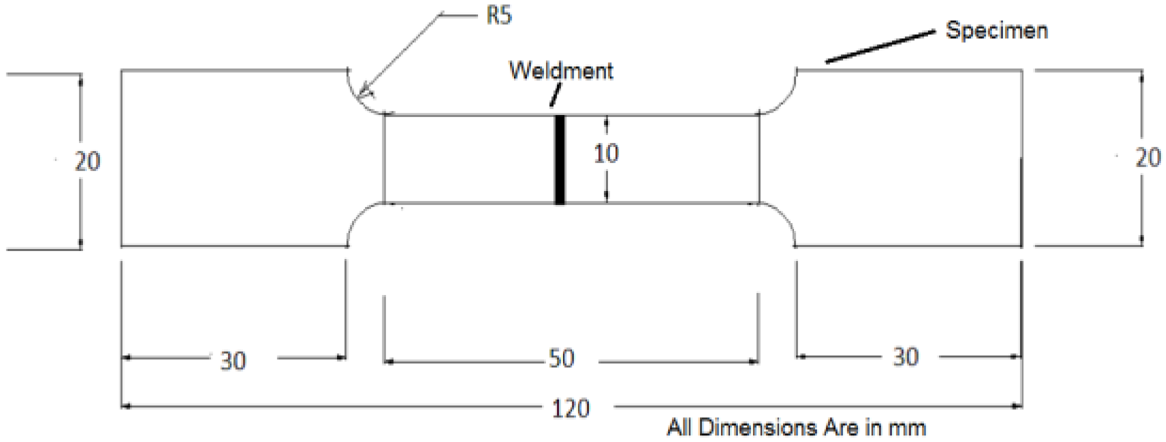

Fig. 3.3 Dimensions of Test Specimen

Fig. 3.4 Sample of Test Specimen

Fig. 3.5 wire cut EDM

3.3. Welding Process:

TIG welding implemented on specimen using a BOIS TIG 200 machine. Tungsten Inert Gas (TIG) welding fuses metal in the joint region and produces a molten weld pool by using the heat generated by an electric arc struck between a non-consumable tungsten electrode and the workpiece. To safeguard the weld pool and non-consumable electrode, the arc area is encased in an inert or reducing gas shield. 2 mm used Tungsten electrode and Argon gas used as shield. Filler can be introduced by introducing a consumable wire or rod into the established weld pool, or the process can be run autogenously (without filler). TIG welds a wide range of materials with thicknesses up to roughly 8 or 10mm and creates very high-quality welds. It works very well with sheet material. Prepared for tensile test, bending test, impact test, total 27 number of welded specimens have been utilised using input parameter 3 level of welding current, 3 level of welding speed 3 level of gas flow rate based on L9 Taguchi's Orthogonal Array in Design of experiment method. The experimentation setup of TIG Welding is shown in Fig. 3.6. Three level and three process parameters such as welding current, welding speed and gas flow rate are selected and the same as Input parameter shown in table 2.

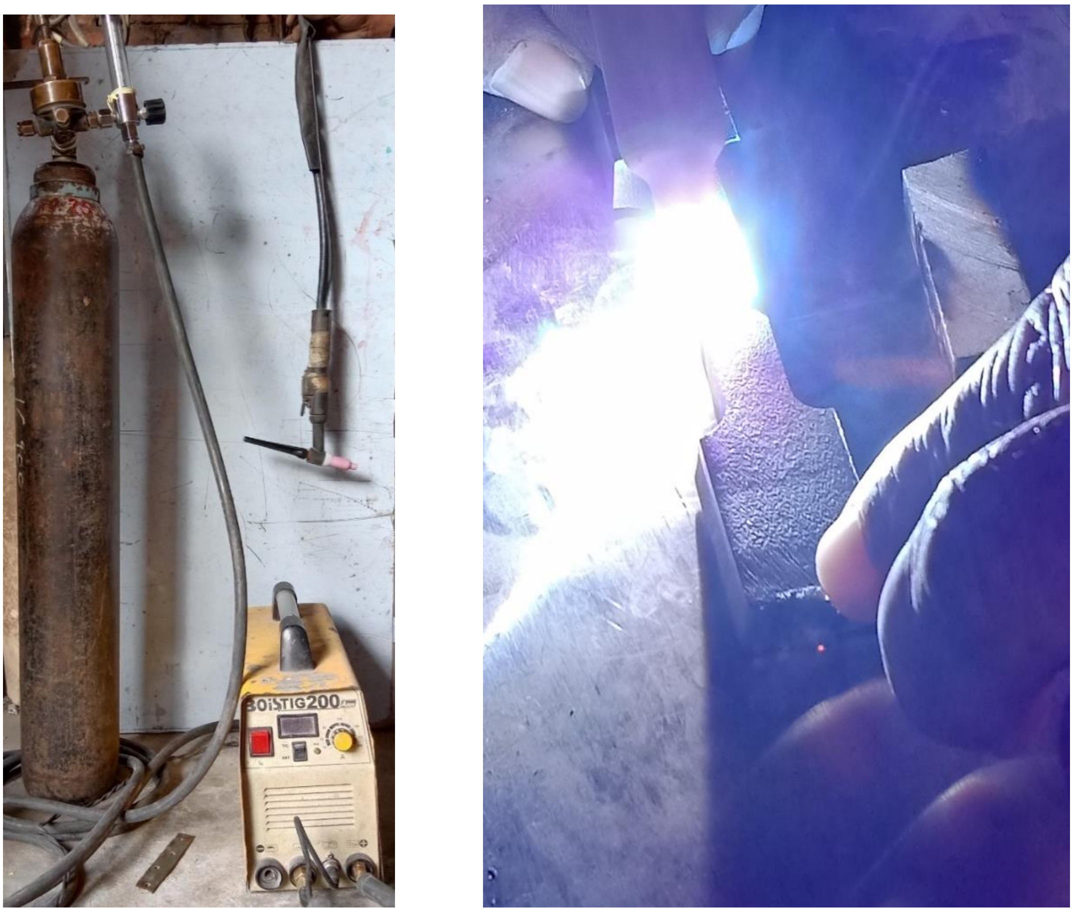

Fig. 3.6 TIG welding setup

After Appling TIG welding the testing specimen shown in fig. 17 And after performed test results shown in table 3.

3.4. Testing:

Tensile test performed on UTM machine and bending test on UTM machine.

And impact test performed on Izod impact test.

3.5. Taguchi optimization:

The optimum TIG welding parameter values have been obtained by the taguchi method. In this analysis the TIG welding characteristics parameters like welding current, welding speed and gas flow rate were set as objective function.

The Taguchi technique of process parameter optimization employs a statistical performance measure known as the signal to noise (S/N) ratio of comparable values of ultimate tensile strength. The S/N ratio is the proportion of the mean (signal) to the standard deviation (noise) (Noise). It is dependent on the product or process quality. The three categories of people, the usual S/N ratio is: i. Nominal the better (NB), ii. larger the better (LB), and iii. lower better (LB). The goal of this project is to maximise tests (output response), hence larger the better (equ.1) has been used.

$$S/N = -10 \times \log_{10}\left(\frac{1}{y_i^2}\right)$$

The multiple s/n ratios (MSRN) have been calculated. These results are listed in table 6. Multiple s/n ratios (MSRN) are listed in table 5. The parameters with MSRN values for responses (welding current, welding speed and gas flow rate) have been plotted. Table 5 that for welding current maximum mean s/n ratio value is obtained at level 3. and welding speed maximum mean s/n ratio value is obtained at level 1. Also, gas flow rate maximum mean s/n ratio value is obtained at level 3.

3.6. Minitab Process:

After performing test then Taguchi optimization design has been implemented in order to identify optimal process parameter with the help of Minitab 19 software. Minitab implementation showing by figures.

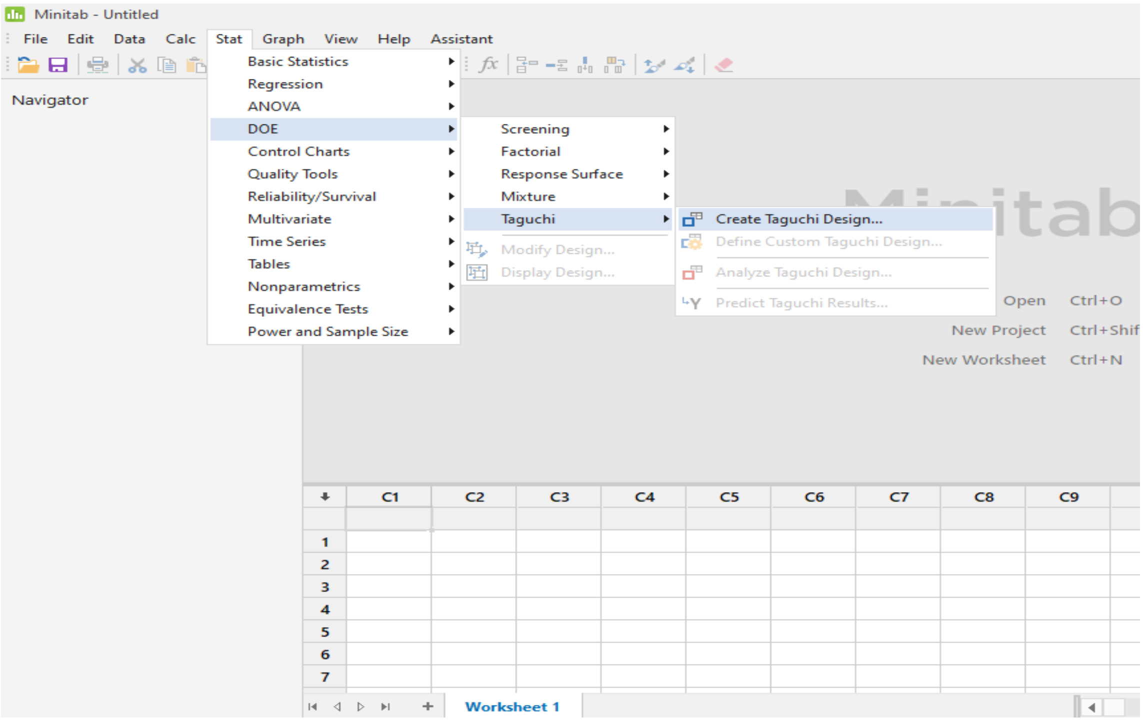

Fig. 3.7 Create taguchi design in Minitab

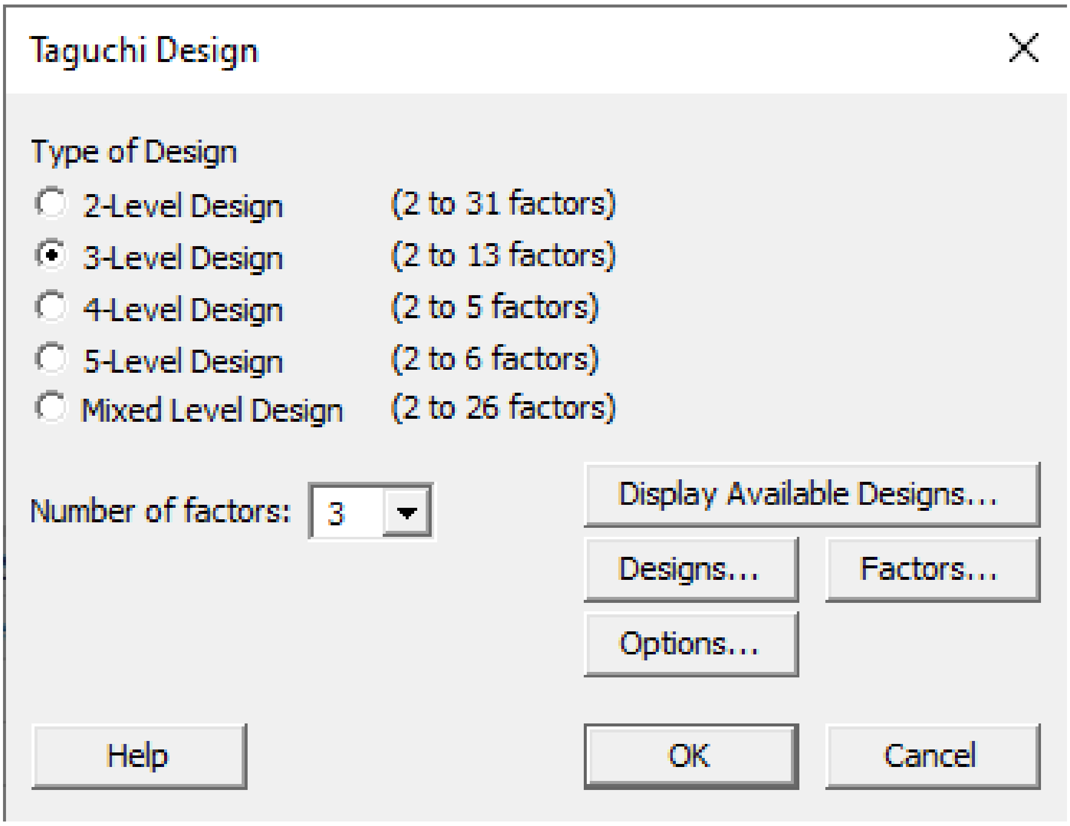

Fig. 3.8 Taguchi design tab

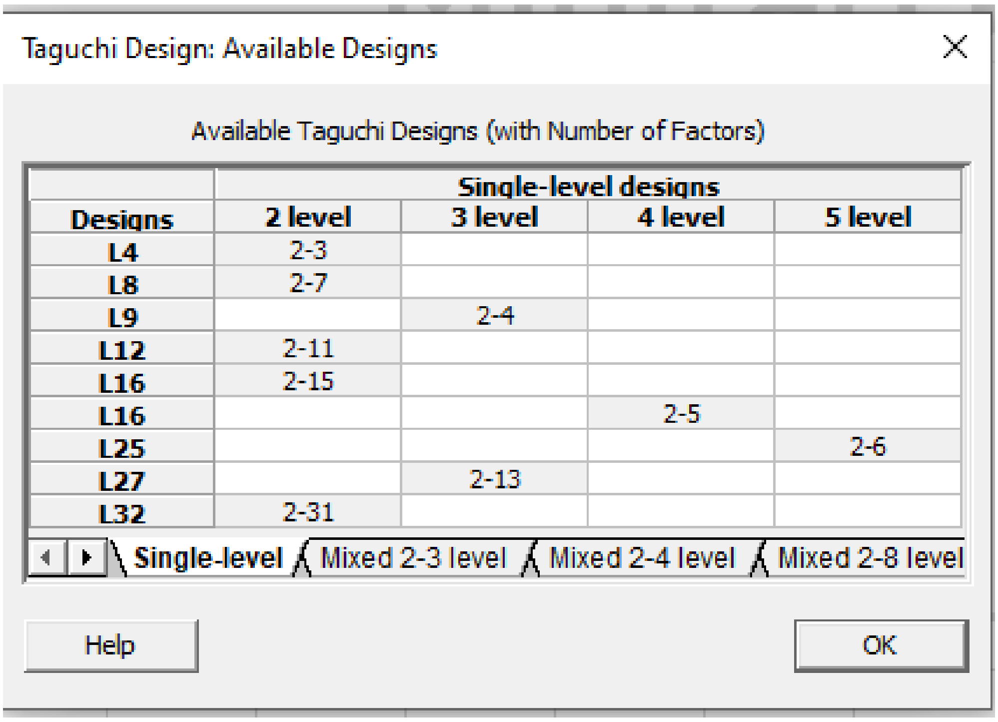

Fig. 3.9 Selection of taguchi design

According to taguchi method select 3x3 matrix it means that L9 orthogonal array. Shown in fig. 3.10.

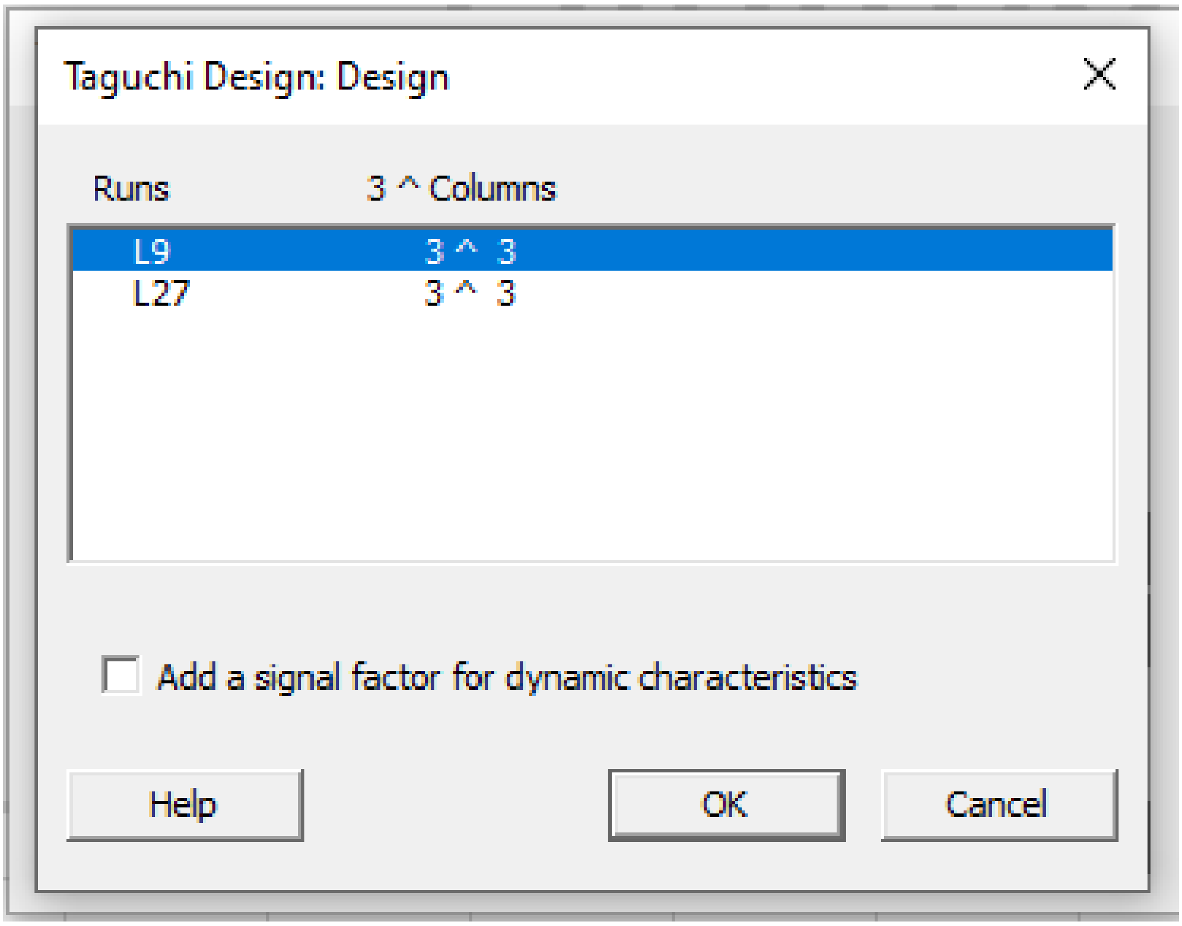

Fig. 3.10 Selection of Array

Table 2 Input parameter

Factor **(Process Parameter)**	**Levels**		
	1	**2**	**3**
Welding Current (Amps)	150	160	170
Welding Speed (mm/Sec)	2	3.5	5
Gas Flow rate(L/min)	10	12	15

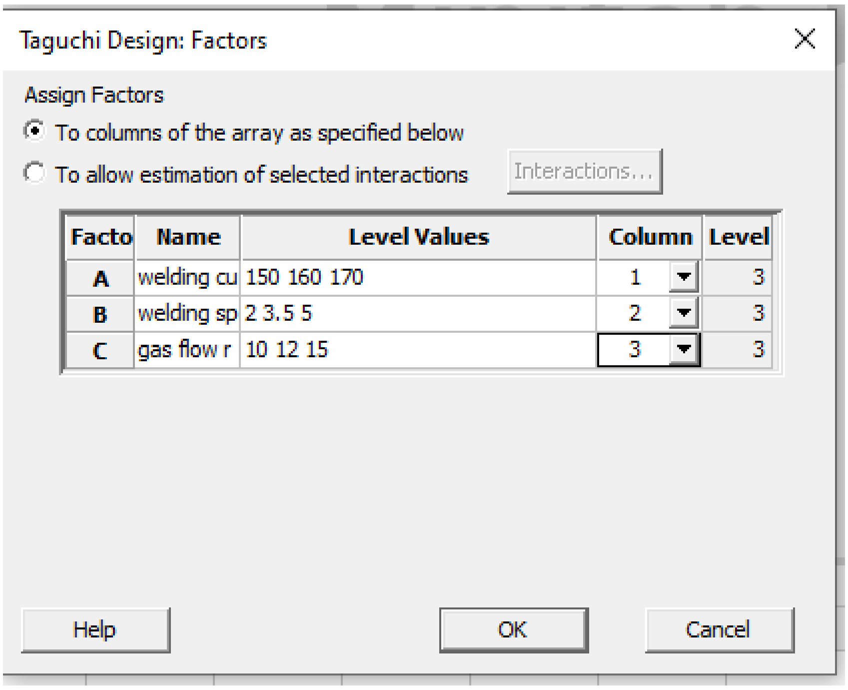

Fig. 3.11 Feeding of level and factors

Feed all input data from table 2 in Minitab, it creates L9 orthogonal array. It is showing this table 3 and fig. 3.11.

Table 3 Orthogonal Array

Factor / Level	Input parameters		
	Welding current (amp)	Welding speed (mm/sec)	Gas flow rate (lit/min)
1	1	1	1
2	1	2	2
3	1	3	3
4	2	1	2
5	2	2	3
6	2	3	1
7	3	1	3
8	3	2	1
9	3	3	2

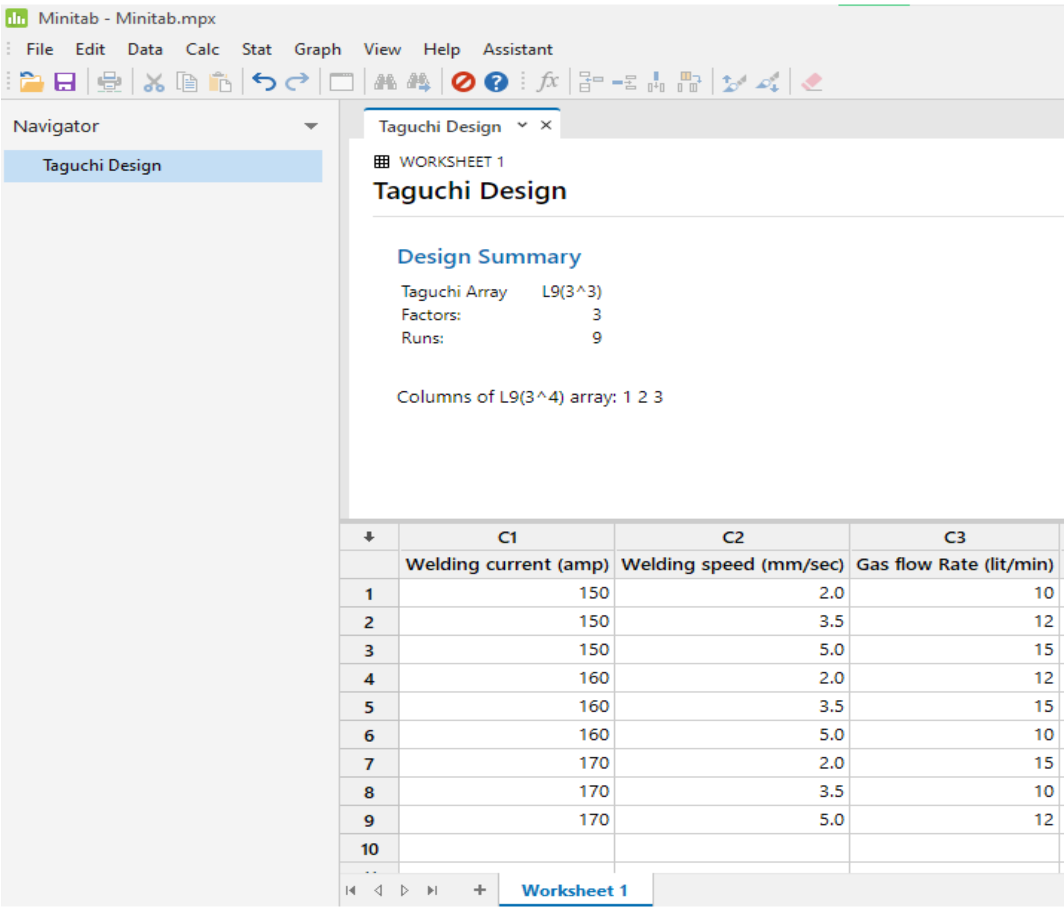

Fig. 3.12 L9 Orthogonal array

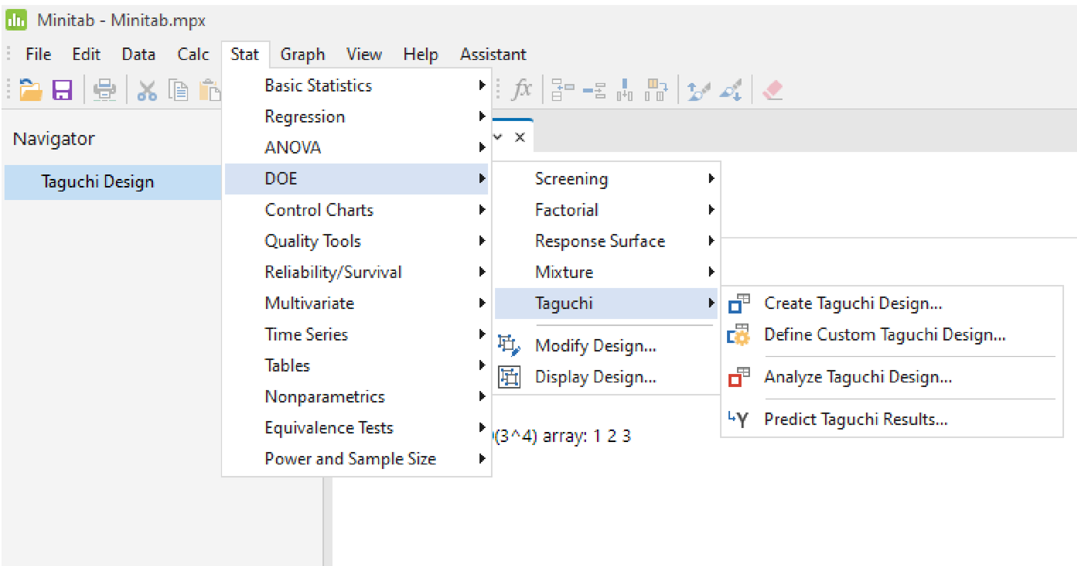

Fig. 3.13 analysing of taguchi design

Analysing taguchi design it's created signal to noise ratio table and graph.

3.7. ANOVA:

The analysis of variance (ANOVA) has been applied as shown in table 4 ANOVA.

Correlative factor (c.f.) = $\frac{(GT)^2}{n}$

Where,

GT = grand total of response

n = no. of observations

Sum of square (SS)= variance of response

Total sum of square = ∑sum of square - cf

Mean square = $\frac{\text{sum of square}}{DOF}$

Percentage contribution (pc) = $\frac{\text{sum of square}}{\text{total sum of square}}$ x 100

F-value = $\frac{MS}{MS_{error}}$

Table 4 Analysis of variance for SN ratios

Source	DF	SS	Pc (%)	MS	F
Welding current (amp)	(n-1)	TRSS-CF	(SS1/TSS) x100	SS1/DF	MS1/MSE
Welding speed (mm/sec)	(n-1)	TRSS-CF	(SS2/TSS) x100	SS2/DF	MS2/MSE
Gas flow rate (lit/min)	(n-1)	TRSS-CF	(SS3/TSS) x100	SS3/DF	MS3/MSE
Residual error	(n-1) (n-2)	TRSS-CF	(SSRE/TSS) x100	SSRE/DF	
Total	(n^2-1)	∑SS			

CHAPTER 4

4 RESULT AND DISCUSSION

4.1. Material:

The material is used in this research work AISI 309 Stainless steel as shown in fig. 4.1.

Fig. 4.1 AISI 309 Stainless Steel

4.2. EDM Process:

Specimen prepared as ASTM standard by EDM wire cutting machine as shown in fig. 4.2, fig. 4.3.

Fig. 4.2 Tensile Testing specimen

Fig. 4.3 Bending Testing specimen

4.3. Welding Process:

The welding process completed as given input parameter from table 2. The welding specimen as shown in below fig. 4.4, fig. 4.5, fig. 4.6.

Fig. 4.4 Welded Testing specimen for tensile tests

Fig. 4.5 Welded Testing specimen For Bending tests

Fig. 4.6 Welded Testing specimen for Impact tests

4.4. Testing:

The tensile test, impact test and bending test specimens performed as per ASTM standard were prepared corresponding to L9 taguchi orthogonal array experiments, have been conducted and the specimens were tested and the results were obtained are given in table 5. From the table 5. the best result is obtained from experiment 7 (ultimate tensile strength = 416.42 MPa, impact strength = 154 Joule, bending strength = 578.22 MPa.) At input parameters (welding current = 170 Amp, welding speed = 2 mm/sec and gas flow rate = 15 lit/min) and the smallest result is obtained from experiment 1 (ultimate tensile strength = 311.85 MPa, impact strength = 90 Joule, bending strength = 436.52 MPa.) At input parameters (welding current = 150 Amp, welding speed = 2 mm/sec and gas flow rate = 10 lit/min).

Table 5 Experimental results using L9 (OA)

Exp. No.	Input parameters			Output parameters		
	Welding current (amp)	Welding speed (mm/sec)	Gas flow rate (lit/min)	Ultimate tensile strength (MPa)	Impact strength (Joule)	Bending strength (MPa)
1	150	2	10	311.85	90	436.52
2	150	3.5	12	339.43	95	439.22
3	150	5	15	385.22	99	512.33
4	160	2	12	362.06	112	447.23
5	160	3.5	15	394.34	139	126.32
6	160	5	10	343.97	103	441.95
7	170	2	15	416.42	154	578.22
8	170	3.5	10	361.62	143	470.51
9	170	5	12	405.66	140	525.34

4.5. Taguchi optimization:

An approach based on the orthogonal array was created by Genchi Taguchi, a Japanese physicist. This method is used to improve the quality of things manufactured. This method is frequently used for the optimization of process parameters in design in order to lower the cost of making items and improve their quality. Employing the DOE (Design of Experiment) in a systematic and valuable method to reduce variability and to give a solid design for the process's manufacturing performance. The procedure for analysing the procedure parameter is a complex and time-consuming process due to the large number of experiments that must be carried out. The number of process parameters grows as the number of process parameters grows. Taguchi technique can be utilised to tackle this problem since it uses an orthogonal array to analyse any number of process parameters with a very small number of experiments. As a result, this strategy decreases the time and effort required by the designer to investigate the effects of many elements. The Taguchi method's key advantage is that it emphasises the mean performance characteristics value that is close to the target value rather than a value within specific restrictions.

4.6. Minitab:

Optimization processes is proceeded by Minitab 19 software as follows:

Table 6 Multiple S/N ratios (MSRN)

Snra1	Snra2	Snra3	MSNR
49.8789	39.0849	52.8001	0.879831
50.6150	39.5545	52.8536	0.913743
51.7142	39.9127	54.1910	0.908343
51.1756	40.9844	53.0106	0.831797
51.9174	42.8603	42.0294	0.891516
50.7304	40.2567	52.9075	0.990000
52.3906	43.7504	55.2419	0.944057
51.1650	43.1067	53.4514	0.964893
52.1632	42.9226	54.4088	0.879831

Table 7 Response for signal to noise ratios

Symbol	Factors	Mean of multiple s/n ratio (db)		
		Level 1	Level 2	Level 3
A	Welding current (amp)	43.80	44.50	47.18*
B	Welding speed (mm/sec)	45.39*	44.89	45.21
C	Gas flow rate (lit/min)	44.90	45.29	45.30*

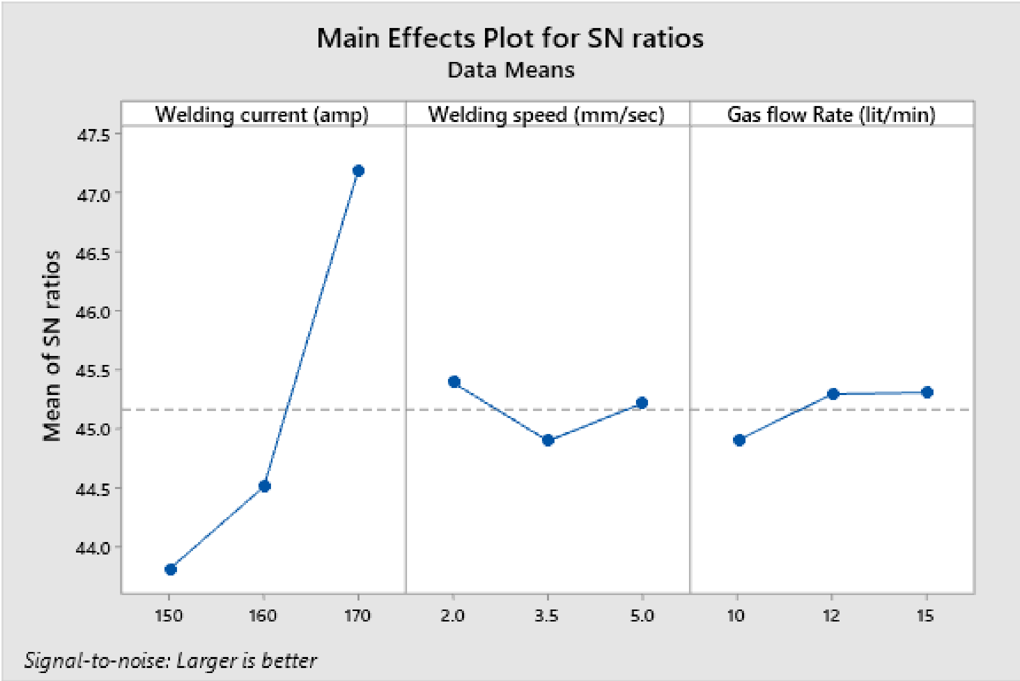

Fig. 4.7 Main effects plot for S/N ratio

Table 7 and fig. 4.7. Show that for WC maximum mean s/n ratio value is achieved at level 3. And WS maximum mean S/N ratio value is achieved at level 3. Also, GFR maximum mean S/N ratio value is achieved at level 3. Hence the optimum value is welding current 170 amp (level 3), welding speed 2mm/sec (level 1) and gas flow rate 15 lit/min (level 3).

4.7. ANOVA:

Analysis of variance (ANOVA) using MINITAB 19 software has been achieved to determine the contribution of input process parameters of TIG welding on ultimate tensile strength for Taguchi design optimization method. From the Table 8 it is found that welding current is the most significant factor. Gas flow rate is not a very significant input process parameter which influences the output tests.

Table 8 Analysis of variance for SN ratios

Source	Df	Ss	Pc (%)	Ms	F
Welding current (amp)	2	19.1054	92.68	9.5527	23.41
Welding speed (mm/sec)	2	0.3784	1.84	0.1892	0.46
Gas flow rate (lit/min)	2	0.3146	1.53	0.1573	0.39
Residual error	2	0.8162	3.96	0.4081	
Total	8	20.6145			

The percentage contribution (pc) of each parameter on responses are as WC-92.68%, WS-1.84% and GFR-1.53% positively.

4.8. Experimental validation:

The higher value of mean MSNR (table 6) represents the exceptional value. The confirmation tests have been executed by supervise a test at central value of the factor and the levels that were calculated previously. The motive is to prove the optimum level suggested by taguchi technique. The experimental results and the predicted values at initial setting of parameters are listed in table 7.

Table 9 Confirmation test using tm technique

Response	Initial setting	Optimum values	% Improvement
		Test	
Level	A_1-b_1-c_1	A_3-b_3-c_3	
(UT) Ultimate tensile strength	311.85	415.90	25.02%
(IT) Impact strength	90.00	153.00	41.18%
(BT) Bending strength	436.52	579.01	24.61%

Table 9 shows that with the experimental values of WC (170 amp), WS (2 mm/sec) and GFR (15 ltr/min), the improvement of 25.02%, 41.18%, 24.61% in UT, IT and BT is found respectively on comparing it with the initial values of WC (150 amp), WS (2 mm/sec) and GFR (10 ltr/min).

CHAPTER 5

5 CONCLUSION AND SCOPE OF FUTURE WORK

5.1. Conclusion:

- With these input parameter (WC 170 A, WS 2 mm/sec and GFR 15 lit/min), the three test were conducted, yielded the best values of output parameter (ultimate tensile strength-416.42 MPa, Impact strength-154 Joule and Bending strength-578.22 MPa). And the input parameter (WC 150 A, WS 2 mm/sec, and GFR 10 lit/min), the three test were conducted, yielded the lowest value of output parameter (ultimate tensile strength-311.85 MPa, impact strength-90 Joule, and bending strength-436.52 MPa).
- The goal of Taguchi's optimization is to enhance ultimate tensile strength (UTS). The Taguchi S/N ratio concept was used, and it was discovered that WC at level 3, WS at level 1, and GFR at level 3 (WC 170 A, WS 15 mm/sec, and GFR 15 l/min) was the optimal process parametric condition of welded specimen for higher values of ultimate tensile strength (UTS).
- The goal of Taguchi's optimization is to enhance Bending strength. The Taguchi S/N ratio concept was used, and it was discovered that WC at level 3, WS at level 1, and GFR at level 3 (WC 170 A, WS 15 mm/sec, and GFR 15 l/min) was the optimal process parametric condition of welded specimen for higher values of Bending strength.
- The goal of Taguchi's optimization is to enhance Impact strength. The Taguchi S/N ratio concept was used, and it was discovered that WC at level 3, WS at level 1, and GFR at level 3 (WC 170 A, WS 15 mm/sec, and GFR 15 l/min) was the optimal process parametric condition of welded specimen for higher values of Impact strength.

- The optimization by taguchi method provides best conditions which get applicable through obtained exceptional responses in confirmatory tests.
- According to the results of the analysis of variance, all of the process parameters, WC, WS, and GFR, contributed significantly with 92.68 percent, 41.18 percent, and 24.61 percent, respectively, and Error Contribution was 3.96 percent.

5.2. Future aspects:

- The using welding parameter in this research work are not enough, we can use various other different parameters also.
- The parameters of the TIG welding process are crucial in determining the quality of a welded connection. So, further research work on welding parameters.
- AISI 309 Stainless steel have more corrosion resistance as compared to AISI 304 Stainless steel. So, it’s used to prevent corrosion from more moisture containing environment.

REFERENCES:

1. Shanmugasundar, g., karthikeyan, b., ponvell, p.s. and vignesh, v., 2019. Optimization of process parameters in TIG welded joints of AISI 304l-austenitic stainless steel using taguchi's experimental design method. *Materials today: proceedings*, *16*, pp.1188-1195.
2. Natrayan, l., anand, r. And kumar, s.s., 2021. Optimization of process parameters in TIG welding of AISI 4140 stainless steel using taguchi technique. *Materials today: proceedings*, *37*, pp.1550-1553.
3. Vinoth, v., sudalaimani, r., ajay, c.v., kumar, c.s. and prakash, k.s., 2021. Optimization of mechanical behaviour of TIG welded 316 stainless steel using taguchi based grey relational analysis method. *Materials today: proceedings*, *45*, pp.7986-7993.
4. Kumar, s., jena, s., lahoty, v., paswan, m.k., sharma, b., patel, d., prasad, s.b. and sharma, v.k., 2020. Experimental investigation on the effect of welding parameters of tig welded joints using ANOVA. *Materials today: proceedings*, *22*, pp.3181-3189.
5. Avinash, s., balram, y., babu, b. S., & venkatramana, g. (2019). Multi-response optimization of pulse tig welding process parameters of welds AISI 304 and monel 400 using grey relational analysis. *Materials today: proceedings*, *19*, 296-301.
6. Ahmad, a. And alam, s., 2019. Integration of rsm with grey based taguchi method for optimization of pulsed tig welding process parameters. *Materials today: proceedings*, *18*, pp.5114-5127.
7. Jayashree, p.k., sharma, s.s., shetty, r., mahato, a. And gowrishankar, m.c., 2018. Optimization of tig welding parameters for 6061al alloy using taguchi's design of experiments. *Materials today: proceedings*, *5*(11), pp.23648-23655.
8. Mishra, d. And dakkili, m., 2020. Gas tungsten and shielded metal arc welding of stainless steel 310 and 304 grades over single and double 'v'butt joints. *Materials today: proceedings*, *27*, pp.772-776.
9. Ramana, m.v., kumar, b.r., krishna, m., rao, m.v. and kumar, v.s., 2020. Optimization and influence of process parameters of dissimilar ss304l–ss430 joints produced by robotic tig welding. *Materials today: proceedings*, *23*, pp.479-482.

10. Modenesi, p.j., apolinario, e.r. and pereira, i.m., 2000. Tig welding with single-component fluxes. *Journal of materials processing technology*, *99*(1-3), pp.260-265.
11. Ghosh, n., pal, p. K., & nandi, g. (2017). Parametric optimization of gas metal arc welding process by pca-based taguchi method on ferritic stainless steel AISI409. *Materials today: proceedings*, *4*(9), 9961-9966.
12. Muhammad, n., manurung, y.h., hafidzi, m., abas, s.k., tham, g. And haruman, e., 2012. Optimization and modeling of spot welding parameters with simultaneous multiple response consideration using multi-objective taguchi method and rsm. *Journal of mechanical science and technology*, *26*(8), pp.2365-2370.
13. Ahirwar, P., 2015. Experimental Investigation on Autogenous Tungsten Inert Gas (TIG) Welding of AISI 1020 Mild Steel (Doctoral dissertation).
14. Abhulimen, I.U. and Achebo, J.I., Prediction of Weld Quality of A Tungsten Inertr Gas Welded Mild Steel Pipe Joint Using Response Surface Methodology (Rsm).
15. Verma, J. and Taiwade, R.V., 2017. Effect of welding processes and conditions on the microstructure, mechanical properties and corrosion resistance of duplex stainless steel weldments—A review. Journal of Manufacturing Processes, 25, pp.134-152.
16. Ahirwar, P., 2015. Experimental Investigation on Autogenous Tungsten Inert Gas (TIG) Welding of AISI 1020 Mild Steel (Doctoral dissertation).
17. chandra siddhardha Allada, S., Sai, P.S., Banala, S., Subbiah, R. and Marichamy, S., 2021. Tensile strength performance and optimization of Al 7068 using TIG welding process. Materials Today: Proceedings, 45, pp.2017-2021.
18. Vikesh, R.J. and Suri, N.M., 2013. Effect of A-TIG welding process parameters on penetration in mild steel plates. International Journal of Mechanical and Industrial Engineering, 3, pp.34-37.
19. Pal, K. and Kumar, V., 2014. Effect of Activated TIG welding on wear properties and dilution percentage in medium carbon steel welds, journal Emerging Technology and advanced Engineering vol. 4.
20. Afolalu, S.A., Soetan, S.B., Ongbali, S.O., Abioye, A.A. and Oni, A.S., 2019, November. Impact of activated–flux tungsten inert gas (a-tig) welding on weld joint

of a metal–Review. In IOP Conference Series: Materials Science and Engineering (Vol. 640, No. 1, p. 012064). IOP Publishing.

21. Dhandha, K.H. and Badheka, V.J., 2015. Effect of activating fluxes on weld bead morphology of P91 steel bead-on-plate welds by flux assisted tungsten inert gas welding process. Journal of Manufacturing Processes, 17, pp.48-57.
22. Fujii, N., Honda, H., Fukase, A. and Yasuda, K., 2007. Comparison of strength characteristics of nodular graphite cast iron welded joints by various welding processes. Welding International, 21(9), pp.634-641.
23. Mahajan, S., Biradar, N.S., Raman, R. and Mishra, S., 2012. Effect of mechanical arc oscillation on the grain structure of mild steel weld metal. Transactions of the Indian Institute of Metals, 65(2), pp.171-177.
24. Pasupathy, J. and Ravisankar, V., 2013. Parametric optimization of TIG welding parameters using Taguchi method for dissimilar joint (low carbon steel with AA1050). International Journal of Scientific & Engineering Research, 4(11), pp.25-28.
25. Aissani, M., Guessasma, S., Zitouni, A., Hamzaoui, R., Bassir, D. and Benkedda, Y., 2015. Three-dimensional simulation of 304L steel TIG welding process: Contribution of the thermal flux. Applied Thermal Engineering, 89, pp.822-832.
26. Nasiri, M.B., Behzadinejad, M., Latifi, H. and Martikainen, J., 2014. Investigation on the influence of various welding parameters on the arc thermal efficiency of the GTAW process by calorimetric method. Journal of Mechanical Science and Technology, 28(8), pp.3255-3261.
27. Meng, X., Qin, G., Zhang, Y., Fu, B. and Zou, Z., 2014. High speed TIG–MAG hybrid arc welding of mild steel plate. Journal of Materials Processing Technology, 214(11), pp.2417-2424.

List of Publications

- My paper entitled "OPTIMIZATION AND MODELLING ON TIG WELDING OF AISI 309 STAINLESS STEEL UNDER VARIOUS WELDING PARAMETER USING TAGUCHI METHOD" is Published under Dogo Rangsang Research Journal UGC Care Group I Journal ISSN: 2347-7180 Vol-09 Issue-01 No. 01: 2022 https://journaldogorangsang.in/no_1_Online_22.html.

- My paper entitled "EXPERIMENTAL STUDIES ON TIG WELDING OF ADVANCED MATERIAL UNDER VARIOUS PARAMETERS" is presented and submitted for acceptance in the International Conference on Processing and Characterization of Materials (ICPCM –22) organized by SSN College of Engineering.

- My paper entitled "EXPERIMENTAL STUDIES ON TIG WELDING OF ADVANCED MATERIAL UNDER VARIOUS PARAMETERS" is accepted and presented in the "International Conference on Advances in Mechanical Engineering-2022" (ICAME-2022) organized by the Department of Mechanical Engineering G H Raisoni College of Engineering, Nagpur, India and is waiting for the publication.

Ouriginal

Document Information

Analyzed document	Safraj thesis for plagiarism.pdf (D140976751)
Submitted	2022-06-22 08:58:00
Submitted by	Amrit Anand Dosar
Submitter email	amritdosar@bbdu.ac.in
Similarity	24%
Analysis address	amritdosar.bbduni@analysis.urkund.com

Sources included in the report

SA	**200650728001 kundan.pdf** Document 200650728001 kundan.pdf (D135611768)	4
W	URL: https://m.scirp.org/papers/87034 Fetched: 2021-05-17 12:09:43	1
W	URL: https://weldingeasy.com/how-does-tig-welding-work/ Fetched: 2022-06-22 08:59:46	1
SA	**Sant Longowal Institute Of E&T / WORD FILE FORMAT.docx** Document WORD FILE FORMAT.docx (D114480784) Submitted by: rakeshsliet@yahoo.co.in Receiver: rakeshsliet.sliet@analysis.urkund.com	1
SA	**Anna University, Chennai / 7086033109-TS.pdf** Document 7086033109-TS.pdf (D19227526) Submitted by: adldirresearch@gmail.com Receiver: adldirresearch.annauniv@analysis.urkund.com	1
SA	**171010709004.docx** Document 171010709004.docx (D103958122)	9
SA	**Madanapalle Institute of Technology & Science / 17695A0331_Microstructual Properties.docx** Document 17695A0331_Microstructual Properties.docx (D73359327) Submitted by: dean-rrc@mits.ac.in Receiver: dean-rrc.mits@analysis.urkund.com	4
SA	**I K Gujral Punjab Technical University, Jalandhar / Rajat_Thesis_Report.doc** Document Rajat_Thesis_Report.doc (D58842920) Submitted by: raminder_212003@rediffmail.com Receiver: raminder_212003.ptu@analysis.urkund.com	10
SA	**RIMT University / THESIS OF SHAH ARJUMAND 20-M-ME-22.docx** Document THESIS OF SHAH ARJUMAND 20-M-ME-22.docx (D138458101) Submitted by: ashishoberoi@rimt.ac.in Receiver: ashishoberoi.rimt@analysis.urkund.com	1
W	URL: http://www.ijies.net/finial-docs/finial-pdf/2611194123.pdf Fetched: 2021-12-06 11:58:15	9

SA **200650728001_kundan.pdf**
Document 200650728001_kundan.pdf (D135727452) 1

SA **200650728001 kundan.pdf**
Document 200650728001 kundan.pdf (D135617640) 13

SA **190750728002.pdf**
Document 190750728002.pdf (D104269905) 2

SA **Anna University, Chennai / 20082062002-TS(CHELLAPPAN M).pdf**
Document 20082062002-TS(CHELLAPPAN M).pdf (D21353770)
Submitted by: ddcfresearch@gmail.com
Receiver: adldirresearch.annauniv@analysis.urkund.com 2

SA **RIMT University / Thesis by Shah Arjumand.pdf**
Document Thesis by Shah Arjumand.pdf (D140585352)
Submitted by: manishgupta@rimt.ac.in
Receiver: manishgupta.rimt@analysis.urkund.com 2

SA **Indian Institute Of Technology, Dhanbad / experimental report.docx**
Document experimental report.docx (D57048781)
Submitted by: somnathchattopadhyaya@iitism.ac.in
Receiver: somnathchattopadhyaya.iitism@analysis.urkund.com 1

W URL: https://www.sciencedirect.com/science/article/pii/S2214785320322355
Fetched: 2021-11-29 09:57:50 1

SA **Govind Ballabh Pant University of Agri. and Tech. / 2-rewiew-updated.docx**
Document 2-rewiew-updated.docx (D140802688)
Submitted by: aruncdme@gmail.com
Receiver: aruncdme.gbuni@analysis.urkund.com 1

W URL: http://ethesis.nitrkl.ac.in/7614/1/2015_Experimental_Pankaj.pdf
Fetched: 2021-10-04 19:04:54 22

SA **Manipal University, Jaipur / yaten 11.pdf**
Document yaten 11.pdf (D53964746)
Submitted by: office.phd@jaipur.manipal.edu
Receiver: office.phd.manj@analysis.urkund.com 3

Entire Document

1 CHAPTER 1 1 INTRODUCTION 1.1. Material AISI 309 stainless steels: Stainless steel (AISI 309) is extensively used in almost all types of thermal power plant, petroleum industries, waste treatment industries etc. This type of AISI 309 has high strength, weldability, toughness, ductility, excellent oxidization resistance and excellent formability. AISI 309 SS applications includes furnace parts, jet engine parts, heat exchangers, evaporators, chemical processing equipment, Automotive exhaust part, tanks, Fire box sheet and Other high temperature Containers. The chemical composition of AISI 309 is show in table 1. And material shown in fig. 1. Table 1 The chemical composition of AISI309 Stainless Steel 309 is an austenitic stainless steel that's frequently utilised in high- temperature applications. Because of the high chromium and nickel content, it has comparable oxidation and corrosion resistance. 309 stainless steel can be machined in the same way that 304 stainless steel can. Grade 309 Stainless Steel can also be welded utilising the resistance and fusion method. Oxyacetylene welding is not advised for welding 347H stainless steel. The 309 stainless steel grade is heated to 1177°C, then reheated to 982°C before being quenched quickly. After-work annealing can be used to restore its corrosion resistance. If the work hardening rate of grade 309 stainless steel is high, it can be stamped, headed, upset, and drawn. After cold working, annealing is performed to minimise internal tension. After annealing at 1038-1121°C, 309 stainless steel is quenched in water. Cold working can improve the hardness and strength of 309 steel. Grade C% Si% Mn% P% S% N% Cr% Ni% 309 0.067 0.26 1.73 0.036 0.003 - 22.15 12.19
2 Fig. 1 Material (AISI 309 Stainless steel) 1.2. TIG Welding of AISI 309 stainless steel: To improve the mechanical qualities of stainless steel, the tungsten inert gas (TIG) welding method is used. TIG welding produces a higher-quality, more accurate weld, a smaller heat

BBD UNIVERSITY

BABU BANARASI DAS UNIVERSITY, LUCKNOW
CERTIFICATE OF FINALTHESIS SUBMISSION

1. Name: …………………………………………………...………………………
2. Enrolment No.: ………………………………………………………….………....
3. Thesis title………….……………………………………...…………………….
   ……….………………………………...……………..………………..…..
   …..………………..…….…………………………………….……………………
4. Degree for which the thesis is submitted: ……………………………………………
5. School (of the University to which the thesis is submitted)
   ………………………………………………………………………………………….
6. Thesis Preparation Guide was referred to for preparing the thesis. ☐YES ☐NO
7. Specifications regarding thesis format have been closely followed. ☐YES ☐NO
8. The contents of the thesis have been organized based on the guidelines. ☐YES ☐NO
9. The thesis has been prepared without resorting to plagiarism. ☐YES ☐NO
10. All sources used have been cited appropriately. ☐YES ☐NO
11. The thesis has not been submitted elsewhere for a degree. ☐YES ☐NO
12. All the corrections have been incorporated. ☐YES ☐NO
13. Submitted 4 hard bound copies plus one CD. ☐YES ☐NO

(Signature(s) of the Supervisor(s))
Name(s): ……………..…………

(Signature of the Candidate)
Name: ……………..………………..
Roll No.: …………………………….
Enrolment No.: ……………………...